Probes for Narcotic Receptor Mediated Phenomena. 34. Synthesis and Structure−Activity Relationships of a Potent μ-Agonist δ-Antagonist and an Exceedingly Potent Antinociceptive in the Enantiomeric C9-Substituted 5-(3-Hydroxyphenyl)-*N*-phenylethylmorphan Series

Anne-Cécile Hiebel,[†,‡] Yong Sok Lee,[⊥] Edward Bilsky,[∞] Denise Giuvelis,[∞] Jeffrey R. Deschamps,[§] Damon A. Parrish,[§] Mario D. Aceto,[¢] Everette L. May,[¢] Louis S. Harris,[¢] Andrew Coop,[||] Christina M. Dersch,[¶] John S. Partilla,[¶] Richard B. Rothman,[¶] Kejun Cheng,[‡] Arthur E. Jacobson,[‡] and Kenner C. Rice*[,‡]

Drug Design and Synthesis Section, Chemical Biology Research Branch, National Institute on Drug Abuse, and Center for Molecular Modeling, Division of Computational Bioscience, Center for Information Technology, National Institutes of Health, DHHS, Bethesda, MD 20892, University of New England, College of Osteopathic Medicine, Biddeford, ME 04005, Laboratory for the Structure of Matter, Naval Research Laboratory, Washington, DC 20375, Department of Pharmacology and Toxicology, School of Medicine, Virginia Commonwealth University, Richmond VA 23298, Department of Pharmaceutical Sciences, University of Maryland School of Pharmacy, Baltimore, MD 21201, and Clinical Psychopharmacology Section, National Institute on Drug Abuse, Addiction Research Center, National Institutes of Health, DHHS, Baltimore, MD 21224

Received November 15, 2006

Both of the enantiomers of 5-(3-hydroxyphenyl)-*N*-phenylethylmorphan with C9α-methyl, C9-methylene, C9-keto, and C9α- and C9β-hydroxy substituents were synthesized and pharmacologically evaluated. Three of the 10 compounds, (1*R*,5*R*,9*S*)-(−)-9-hydroxy-5-(3-hydroxyphenyl-2-phenylethyl-2-azabicyclo[3.3.1]-nonane ((1*R*,5*R*,9*S*)-(−)-**10**), (1*R*,5*S*)-(+)-5-(3-hydroxyphenyl)-9-methylene-2-phenethyl-2-azabicyclo[3.3.1]-nonane ((1*R*,5*S*)-(+)-**14**), and (1*R*,5*S*,9*R*)-(−)-5-(3-hydroxyphenyl)-9-methyl-2-phenethyl-2-azabicyclo-[3.3.1]nonane ((1*R*,5*S*,9*R*)-(+)-**15**) had subnanomolar affinity at μ-opioid receptors (K_i = 0.19, 0.19, and 0.63 nM, respectively). The (1*R*,5*S*)-(+)-**14** was found to be a μ-opioid agonist and a μ-, δ-, and κ-antagonist in [^{35}S]GTP-γ-S assays and was approximately 50 times more potent than morphine in a number of acute and subchronic pain assays, including thermal and visceral models of nociception. The (1*R*,5*R*,9*S*)-(−)-**10** compound with a C9-hydroxy substituent axially oriented to the piperidine ring (C9β-hydroxy) was a μ-agonist about 500 times more potent than morphine. In the single-dose suppression assay, it was greater than 1000 times more potent than morphine. It is the most potent known phenylmorphan antinociceptive. The molecular structures of these compounds were energy minimized with density functional theory at the B3LYP/6-31G* level and then overlaid onto (1*R*,5*R*,9*S*)-(−)-**10** using the heavy atoms in the morphan moiety as a common docking point. Based on modeling, the spatial arrangement of the protonated nitrogen atom and the 9β-OH substituent in (1*R*,5*R*,9*S*)-(−)-**10** may facilitate the alignment of a putative water chain enabling proton transfer to a nearby proton acceptor group in the μ-opioid receptor.

The 5-(3-hydroxy)phenylmorphan class of opioids (3-(2-azabicyclo[3.3.1]nonan-5-yl)phenol, **1a**, Figure 1) was originally synthesized over 50 years ago by May and Murphy,[1] and this type of molecular structure is still of considerable current interest.[2−8] Our interest in the phenylmorphan template has been enhanced by our finding[4,9] that *N*-phenylethyl substitution (**1b**, Figure 1) apparently transforms both enantiomers of **1a** from agonists into antagonists, as determined in [^{35}S]GTP-γ-S assays, and that suitable modification of a phenylmorphan can provide a compound with both μ-agonist and δ-antagonist activity.[10] This combination of receptor interactions in the peptide family of opioid-like agonists and antagonists has been noted to produce analgesia with less tolerance and dependence.[11]

The 1*S*,5*R* enantiomer of **1b** (Figure 1) was a fairly potent μ-, δ-, and κ-opioid antagonist, more potent than the 1*R*,5*S* enantiomer that was found to be a μ- and κ-antagonist.[4,9] We noted that these compounds appeared to be less potent than a racemic mixture that was formerly reported[12] with a C9β-methyl substituent, (±)-5-(3-hydroxyphenyl)-9β-methyl-2-(2′-phenylethyl)-2-azabicyclo[3.3.1]nonane (**1c**), and we stated that the potency difference, rather than the antagonist activity, was more reasonably ascribed to the formerly proposed hindered rotation of the 5-hydroxyphenyl ring.

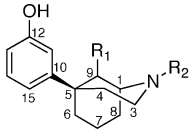

1a: R_1 = H, R_2 = H
1b: R_1 = H, R_2 = CH_2CH_2Ph
1c: R_1 = CH_3, R_2 = CH_2CH_2Ph

Figure 1. Structures of racemic phenylmorphans.

The molecular conformation of the 5-(3-hydroxy)phenylmorphan is different from that of the morphinans, 4,5-epoxymorphinans and 6,7-benzomorphans, because its phenolic ring is equatorially oriented on the piperidine ring, not constrained axially as in these other classes of opioids. Yet many 5-(3-hydroxy)phenylmorphan derivatives show opioid-like in vitro and in vivo activities, and others are opioid antagonists. The different spatial positions of the aromatic rings of the phenyl-

* To whom correspondence should be addressed. Telephone: 301-496-1856. Fax: 301-402-0589. E-mail: kr21f@nih.gov.
† Current address: Provid Pharmaceuticals, Inc., 671 US Highway 1, North Brunswick, NJ 08902.
‡ This work was initiated while these authors were members of the Drug Design and Synthesis Section, Laboratory of Medicinal Chemistry, National Institute of Diabetes, Digestive and Kidney Diseases, NIH.
⊥ Center for Molecular Modeling.
∞ University of New England.
§ Laboratory for the Structure of Matter.
¢ Department of Pharmacology and Toxicology.
|| Department of Pharmaceutical Sciences.
¶ Clinical Psychopharmacology Section.

10.1021/jm061325e CCC: $37.00
Published on Web 07/11/2007

Scheme 1

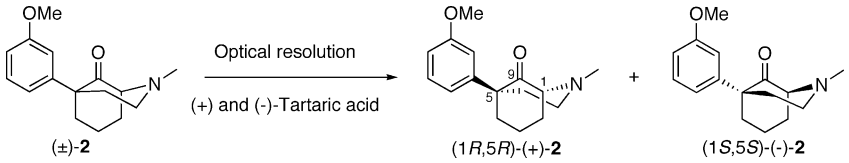

morphans and the morphinans and the wide-range of molecular structures that interact with the μ-opioid receptor have made it difficult to find a reasonable hypothesis that could relate their molecular structures to pharmacological activity either quantitatively or qualitatively.

Because racemic **1c**[12] showed good affinity for opioid receptors ($K_i = 3$ nM) and displayed naltrexone-like nonselective antagonist activity in ex vivo experiments, we thought that it might be of interest to examine other substituents at the C9 position to see what effect they would have on the affinity and selectivity of the 5-phenylmorphan. Thus, we have synthesized both enantiomers of five derivatives of 5-(3-hydroxyphenyl)-*N*-phenylethylmorphan with various substituents at C9. These were the 9α-methyl, the 9-methylene, the 9-keto, and the 9α- and 9β-hydroxy compounds. Two of them, the 9β-hydroxy ((1*R*,5*R*,9*S*)-(−)-**10**) and the 9-methylene ((1*R*,5*S*)-(+)-**14**) derivatives, were found to be especially interesting. The former was found to be extraordinarily potent as an antinociceptive, and the latter was found to be a μ-agonist and a μ-, δ- and κ-antagonist.

Chemistry

Phenylmorphans (1*R*,5*R*)-(+)-**6**, (1*R*,5*R*,9*R*)-(+)-**8**, (1*R*,5*R*,9*S*)-(−)-**10**, (1*R*,5*S*)-(+)-**14**, and (1*R*,5*S*,9*R*)-(+)-**15** and their enantiomers (1*S*,5*S*)-(−)-**6**, (1*S*,5*S*,9*S*)-(−)-**8**, (1*S*,5*S*,9*R*)-(+)-**10**, (1*S*,5*R*)-(−)-**14**, and (1*S*,5*R*,9*S*)-(−)-**15**, stemmed from common intermediates (1*R*,5*R*)-(+)-5-(3-methoxyphenyl)-9-oxo-2-phenylethyl-2-azabicyclo[3.3.1]nonane ((1*R*,5*R*)-(+)-**5**) and its enantiomer (1*S*,5*S*)-(−)-**5**, respectively. The desired enantiomers of **5** were prepared from (±)-**2**. The racemic compound **2** was obtained in nine steps (23.8% overall yield) from commercially available reagents using literature procedures.[1,2] The enantiomers of **2**, (1*R*,5*R*)-(+)-**2** and (1*S*,5*S*)-(−)-**2**, were obtained by selective salt formation with D-(−)- and L-(+)-tartaric acid (Scheme 1). The absolute configuration of the tartrate salt of (1*S*,5*S*)-(−)-**2** was determined by single-crystal X-ray analysis, based on the configuration of the known tartaric acid used for the preparation of the salt (Figure 2).

Initial crystallization of the L-(+)-tartaric acid salt gave an enantiomeric excess of 85% for (−)-**2**, as determined by NMR, with the use of a chiral shift reagent, *R*-(−)-1-phenyl-2,2,2-trifluoroethanol.[13] Recrystallization of the tartrate salt gave (1*S*,5*S*)-5-(3-methoxyphenyl)-2-methyl-9-oxo-2-azabicyclo[3.3.1]-nonane ((1*S*,5*S*)-(−)-**2**) in an enantiomeric excess greater than 99% by NMR. The (1*R*,5*R*)-(+)-**2** enantiomer was obtained in the same manner by crystallization with the other antipode of tartaric acid. Having both enantiomers in hand, the *N*-methyl substituent was replaced by *N*-phenylethyl (Scheme 2). This was achieved via the carbamates ethyl-5-(3-methoxyphenyl)-9-oxo-2-azabicyclo[3.3.1]nonane-2-carboxylate, (1*R*,5*R*)-(+)-**3** and its enantiomer (1*S*,5*S*)-(−)-**3**. For example, the secondary amine (1*R*,5*R*)-5-(3-methoxyphenyl)-9-oxo-2-azabicyclo[3.3.1]-nonane ((1*R*,5*R*)-(−)-**4**) was obtained in good yield after careful treatment with trimethylsilyliodide.[14,15] Alkylation gave the desired *N*-phenylethyl substituent in nearly quantitative yield ((1*R*,5*R*)-5-(3-methoxyphenyl)-9-oxo-2-phenylethyl-2-azabicyclo-

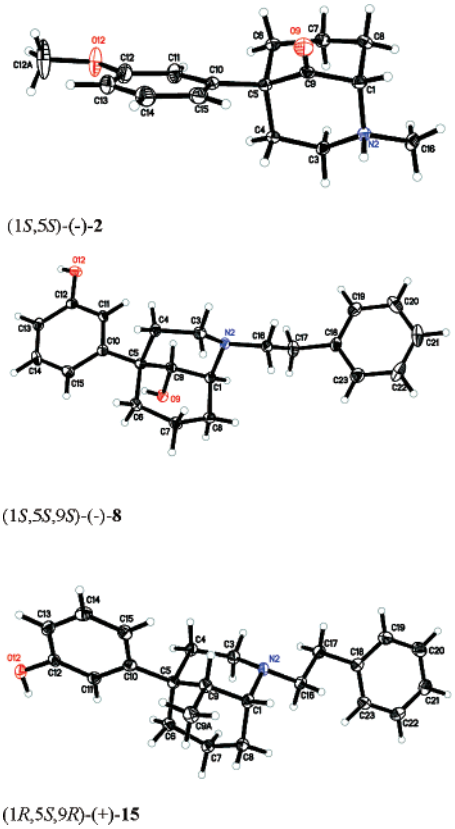

Figure 2. X-ray crystallographic structures of (1*S*,5*S*)-5-(3-methoxyphenyl)-2-methyl-9-oxo-2-azabicyclo[3.3.1]nonane ((1*S*,5*S*)-(−)-**2**), (1*S*,5*S*,9*S*)-(−)-9-hydroxy-5-(3-hydroxyphenyl-2-phenylethyl-2-azabicyclo-[3.3.1]nonane ((1*S*,5*S*,9*S*)-(−)-**8**), and (1*R*,5*S*,9*R*)-(+)-5-(3-hydroxyphenyl)-9-methyl-2-phenethyl-2-azabicyclo[3.3.1]nonane ((1*R*,5*S*,9*R*)-(+)-**15**).

Scheme 2[a]

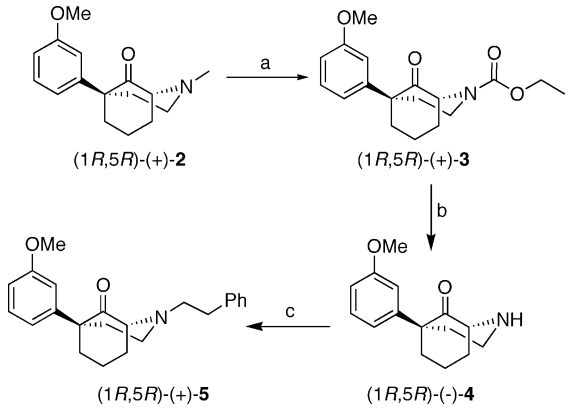

[a] Reagents and conditions: (a) ethylchloroformate, K_2CO_3, 1,2-dichloroethane, 87%; (b) TMSI, 1,2-dichloroethane, 50 °C, 72%; (c) phenylethylbromide, K_2CO_3, KI, acetonitrile, 95%.

[3.3.1]nonane ((1*R*,5*R*)-(+)-**5**)). The enantiomers (1*S*,5*S*)-(+)-**4** and (1*S*,5*S*)-(−)-**5** were prepared similarly.

The intermediate (1*R*,5*R*)-5-(3-hydroxyphenyl)-9-oxo-2-phenylethyl-2-azabicyclo[3.3.1]nonane ((1*R*,5*R*)-(+)-**6**; Scheme 3)

Scheme 3[a]

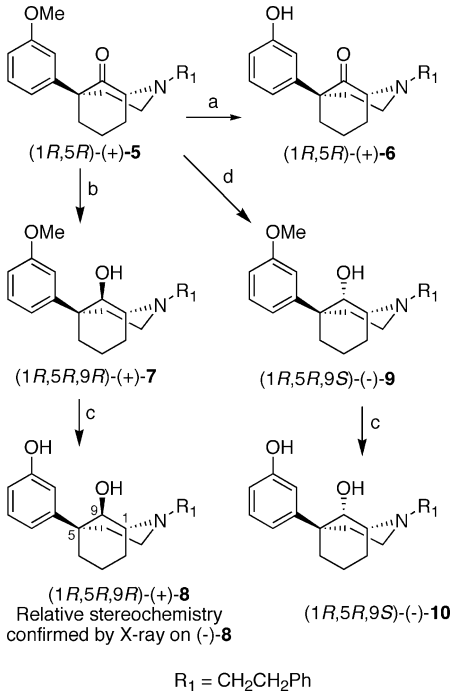

[a] Reagents and conditions: (a) HBr, AcOH, reflux, 75%; (b) $NaBH_4$, MeOH, 90%; (c) BBr_3, CH_2Cl_2, 72−96%; (d) superhydride, THF, 97%.

Scheme 4[a]

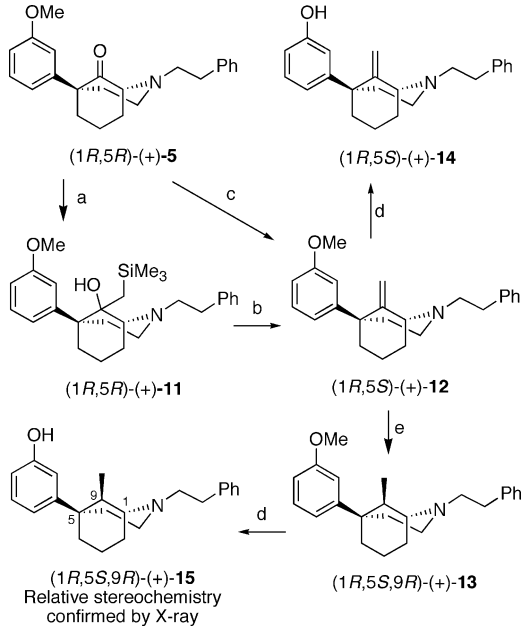

[a] Reagents and conditions: (a) TMS−CH_2MgCl, THF, 92%; (b) NaH, THF, reflux, 98%; (c) Tebbe's reagent,[18,19] THF, 0 °C to room temperature, 75%; (d) BBr_3, CH_2Cl_2, 72−96%; (e) H_2, methanol, 93%.

was obtained by demethylation of the aryl methoxy group of (1*R*,5*R*)-(+)-**5**. Alcohols (1*R*,5*R*,9*R*)-(+)-**8** and (1*R*,5*R*,9*S*)-(−)-**10** were obtained selectively via either sodium borohydride[16] or lithium triethyl borohydride (superhydride)[16] reduction, respectively, followed by demethylation.[17]

Two less polar compounds than (1*R*,5*R*,9*S*)-(−)-**10**, the (1*R*,5*S*)-(+)-**14** and (1*R*,5*S*,9*R*)-(+)-**15** (Scheme 4), were synthesized from the exocyclic methylene compound (1*R*,5*S*)-(+)-**12**. The transformation leading to phenylmorphan (1*R*,5*S*)-(+)-**12** was successful using either Tebbe's reagent[18,19] or Peterson olefination[20] conditions, and the latter gave higher yields. The phenylmorphan enantiomers (1*S*,5*S*)-(−)-**6**, (1*S*,5*S*,9*S*)-(−)-**8**, (1*S*,5*S*,9*R*)-(+)-**10**, (1*S*,5*R*)-(−)-**14**, and (1*S*,5*R*,9*S*)-(−)-**15** were synthesized in the same manner as their antipodes, starting from (1*S*,5*S*)-(−)-**2**.

All of the final 10 enantiomers were purified by radial PLC and recrystallization of their salts (HCl or oxalate). The relative stereochemistries of compounds (1*S*,5*S*,9*S*)-(−)-**8** and (1*R*,5*S*,9*R*)-(+)-**15** were confirmed by single-crystal X-ray crystallography (Figure 2).

Table 1. [125I]Ioxy Binding Data for C9-Substituted 5-Hydroxyphenylmorphans[a]

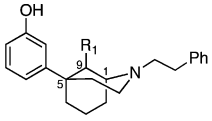

		Ki (nM ± SD)		
C-9 (R_1)	**Compound**	**μ Receptor**	**δ Receptor**	**κ Receptor**
=O	1*S*,5*S*-(-)-**6**	400 ± 23	4600 ± 300	3830 ± 180
=O	1*R*,5*R*-(+)-**6**	33 ± 2	770 ± 40	150 ± 6
−OH	1*S*,5*S*,9*S*-(-)-**8**	45 ± 4	720 ± 40	690 ± 30
−OH	1*R*,5*R*,9R-(+)-**8**	59 ± 3	1570 ± 110	245 ± 8
➡OH	1*R*,5R,9*S*-(-)-**10**	0.19 ± 0.01	13 ± 1.0	184 ± 9
➡OH	1*S*,5*S*,9*R*-(+)-**10**	54 ± 3	2735 ± 315	235 ± 9
$=CH_2$	1*S*,5*R*-(-)-**14**	7 ± 0.4	234 ± 21	18 ± 1
$=CH_2$	1*R*,5*S*-(+)-**14**	0.19 ± 0.01	15 ± 2	0.65 ± 0.04
$-CH_3$	1*S*,5*R*,9*S*-(-)-**15**	8 ± 0.6	300 ± 34	15 ± 1
$-CH_3$	1*R*,5*S*,9*R*-(+)-**15**	0.6 ± 0.1	90 ± 10	4 ± 0.2
➡CH_3	Racemate[b]	3.1 ± 0.2	270 ± 30	14.5 ± 1

[a] [125I]IOXY binding was performed using CHO cells that were stably transfected with either human μ-, δ-, or κ-DNA and express the human μ-, δ-, or κ-opioid receptor, respectively. All results are ±SD, $n = 3$. [b] See ref 3.

Biological Results and Discussion

Initial binding assays in human cells (Table 1) using 125I-IOXY indicated that (1*R*,5*R*,9*S*)-(−)-**10**, (1*R*,5*S*)-(+)-**14**, and (1*R*,5*S*,9*R*)-(+)-**15** had extremely high affinity (subnanomolar) at the μ-receptor. Both (1*R*,5*R*,9*S*)-(−)-**10** and (1*R*,5*S*)-(+)-**14** had good affinity at the δ-receptor, and the latter had subnanomolar affinity at the κ-receptor as well; (1*R*,5*S*,9*R*)-(+)-**15** also had good affinity at the κ-receptor. The enantiomers of these three compounds showed less affinity at opioid receptors, although (1*S*,5*R*)-(−)-**14** and (1*S*,5*R*,9*S*)-(−)-**15** had good affinity (<10 nM) at μ- and a little less affinity at κ-receptors. It is interesting to note that all of the C9-oxygen-containing compounds had at least 10-fold less affinity at κ-receptors than the C9-alkyl or alkylidene compounds. The three most interesting compounds, (1*R*,5*R*,9*S*)-(−)-**10**, (1*R*,5*S*)-(+)-**14**, and (1*R*,5*S*,9*R*)-(+)-**15** were further evaluated in [35S]GTP-γ-S assays, using CHO cells. The (1*R*,5*S*)-(+)-**14** appeared to be a very interesting μ-agonist and a μ-, δ-, and κ-antagonist in the [35S]GTP-γ-S assay, while (1*R*,5*R*,9*S*)-(−)-**10**, the C9β-hydroxy compound

Table 2. Functional Data ([^{35}S]GTP-γ-S)[a]

	μ-agonism E_{max} %[b]	ED_{50} (nM)	δ-agonism E_{max}	ED_{50} (nM)	κ-agonism E_{max}	ED_{50} (nM)
(1*R*,5*R*,9*S*)-(−)-**10**	117 ± 2	5.0 ± 0.5	73 ± 3	341 ± 79	n.d.	n.d.
(1*R*,5*S*)-(+)-**14**	38 ± 1	2.7 ± 0.3	n.d.	n. d.	n.d.	n.d.
(1*R*,5*S*,9*R*)-(+)-**15**	14 ± 1	8.7 ± 2.2	n.d.	n.d.	n.d.	n.d.
morphine	86 ± 3	37 ± 6				
DAMGO	100 ± 3	42 ± 4				
SNC-80			100 ± 4	26 ± 4		

	μ-antagonism K_e[c] (nM)	δ-antagonism K_e[d] (nM)	κ-antagonism K_e[d] (nM)
(1*R*,5*R*,9*S*)-(−)-**10**	n.d.	n.d.	610 ± 120
(1*R*,5*S*)-(+)-**14**	2.2 ± 0.6	12 ± 2	2.0 ± 0.2
(1*R*,5*S*,9*R*)-(+)-**15**	4.4 ± 0.7	31 ± 5	6.0 ± 0.3
naloxone	2.3 ± 0.3		
naltrindole		0.18 ± 0.01	
norBNI			0.11 ± 0.02

[a] [^{35}S]GTP-γ-S binding was performed using CHO cells stably transfected with human μ-, δ-, or κ-cDNA and that stably express μ-, δ-, or κ-opiate receptors; n.d. = not determined. [b] The E_{max} is the extrapolated maximal stimulation where 100% is defined as the stimulation produced by 1 μM DAMGO (465 ± 13 for μ-receptors) and 500 nM SNC80 (425 ± 15 for δ-receptors). In initial screening experiments, no compound had κ-agonist activity. [c] For μ-receptors, K_e values were calculated according to the equation: [test drug]/(EC_{50-2}/EC_{50-1} − 1), where EC_{50-2} is the EC_{50} value of DAMGO in the presence of a fixed concentration of the test drug and EC_{50-1} is the value in the absence of the test drug. [d] For δ- and κ-receptors, K_e values were determined as described in the section Data Analysis and Statistics. Each parameter value is ±SD.

(the hydroxyl moiety was axially oriented in the piperidine ring), displayed agonist activity at μ- and δ-receptors and was a weak κ-antagonist (Table 2). The (1*R*,5*S*,9*R*)-(+)-**15**, bearing an α-methyl substituent at C9 (equatorially oriented on the piperidine ring), showed δ- and κ-antagonist activity and was a weaker μ-agonist than the other two compounds in the [^{35}S]-GTP-γ-S assay. The two more interesting compounds from the functional studies were further evaluated in standard antinociceptive assays in mice, and (1*R*,5*R*,9*S*)-(−)-**10** was found to be over 470 times more potent than morphine in the hot plate and tail flick assays and 200-fold more potent in the PPQ assay, the most potent known phenylmorphan in these assays. In the single-dose suppression assay in the rhesus monkey, this compound completely suppressed morphine abstinence at doses of 0.005 and 0.03 mg/kg and was more than 1000 times more potent than morphine. The (1*R*,5*S*)-(+)-**14** analogue was over 50 times more potent than morphine in the hot plate and tail flick and 17-fold more potent in the PPQ assay in mice. The potency of (1*R*,5*S*)-(+)-**14** as an antinociceptive was corroborated by a 55 °C warm water tail-flick test in mice. The compound produced dose- and time-related antinociceptive effects in this assay following subcutaneous administration. Peak antinociception occurred between 30 and 45 min postinjection, and effects were present at 180 min following a 1 mg/kg dose (Figure 3). The calculated A_{50} value (and 95% confidence limits) for (1*R*,5*S*)-(+)-**14** was 0.11 (0.09−0.15) mg/kg. For comparison purposes, s.c. morphine produced an A_{50} value of 5.95 (5.08−6.95) mg/kg. Thus, the C9β-hydroxy analogue was also about 50-fold more potent than morphine in this assay. The effects of (1*R*,5*S*)-(+)-**14** were blocked by pretreatment with the opioid antagonist naloxone (1 mg/kg, s.c., −10 min, data not shown). Both (1*R*,5*R*,9*S*)-(−)-**10** and (1*R*,5*S*)-(+)-**14** appear to act as potent μ-agonists in vivo, and neither showed μ-antagonist activity in the tail flick versus morphine assay. The potential δ-opioid antagonist profile could not be ascertained in the mouse antinociceptive assays.

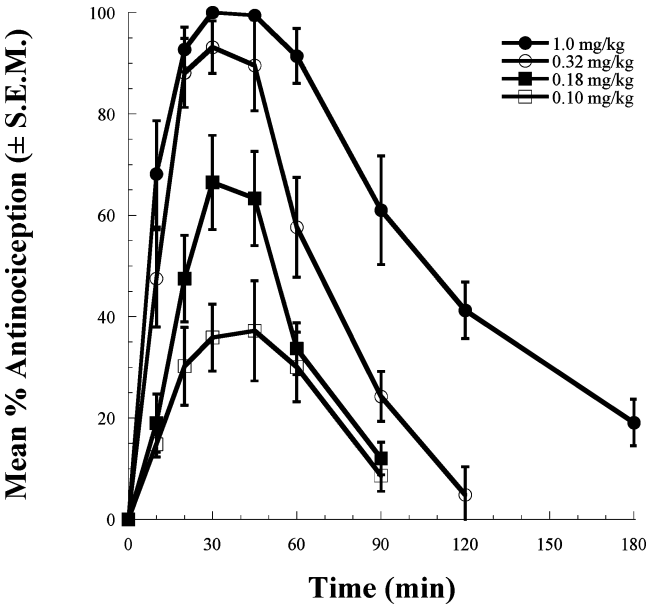

Figure 3. Dose- and time-response curve for subcutaneous (1*R*,5*S*)-(+)-**14** in the 55 °C tail-flick test.

Quantum Chemistry

Agonist versus Antagonist Activity. Rotation of the 5-Hydroxyphenyl Ring of (1*R*,5*R*,9*S*)-(−)-10, (1*R*,5*S*)-(+)-14, and (1*R*,5*S*,9*R*)-(+)-15. The antagonist property of **1c** was rationalized by assuming hindered rotation of the phenolic group around the C5−C10 bond (see Figure 1 for numbering) due to the β-oriented methyl substituent at C9. However, compound **1b**, without a C9 substituent, is also a pure antagonist in the [^{35}S]GTP-γ-S assay, and (1*R*,5*R*,9*S*)-(−)-**10**, (1*R*,5*S*)-(+)-**14,** and (1*R*,5*S*,9*R*)-(+)-**15** with a β-OH, methylene, and α-methyl, respectively, at C9 are agonists. The latter two compounds are not as effective agonists as (1*R*,5*R*,9*S*)-(−)-**10** and show potent antagonist activity in the [^{35}S]GTP-γ-S assay (Table 2). However, (1*R*,5*S*)-(+)-**14** does not show any antagonist activity in vivo, presumably due to its high intrinsic efficacy (Table 3). Thus, the transition from agonist to antagonist is very dependent on the nature and stereochemistry of the substituent at C9 in the *N*-phenethyl-5-hydroxyphenylmorphan series. To probe the previously assumed determinant for imparting the agonist/antagonist property (steric hindrance), the geometries of all the compounds in Table 1 as well as one of the enantiomers of **1b** (1*R*,5*S*) were optimized with density functional theory at the B3LYP/6-31G* level.

Table 3. In Vivo Assays[a]

cmpd	HP	PPQ	TF	TF vs M (mg/kg)	SDS (mg/kg)
(1*R*,5*R*,9*S*)-(−)-10	0.002 (0.001−0.003)[b]	0.002 (0.001−0.004)[b]	0.004 (0.003−0.006)[c]	inactive[c] (1)	CS (0.006−0.03)[d]
(1*R*,5*S*)-(+)-14	0.02 (0.01−0.04)[e]	0.02 (0.016−0.03)[e]	0.03 (0.02−0.04)[f,g]	inactive[f] (1, 10, 30)	CS (0.75−1.0)[h]
morphine·SO_4	0.85 (0.39−1.9)	0.4 (0.2−0.8)	1.92 (0.89−4.14)	inactive (1, 10, 30)	CS (3.0)

[a] ED_{50}, mg/kg, sc (95% confidence limits); HP = hot plate assay, PPQ = phenylquinone assay, and TF = tail flick assay, in mice. The TF vs M = tail flick vs morphine (μ-antagonist assay) in mice; SDS = single dose suppression in monkeys, and CS = complete suppression. Vehicle 5% hydroxypropyl-β-cyclodextrin in H_2O for injection. [b] Highest dose tested was 0.01 mg/kg. [c] Straub tail, ataxia, quick onset, increased locomotor activity, and convulsions were noted at 1 mg/kg. [d] Potency estimate > 1000× morphine. [e] Highest dose tested was 0.1 mg/kg. [f] Straub tail, increased locomotor activity. [g] Highest dose tested was 1 mg/kg. [h] Potency estimate was about 3× morphine.

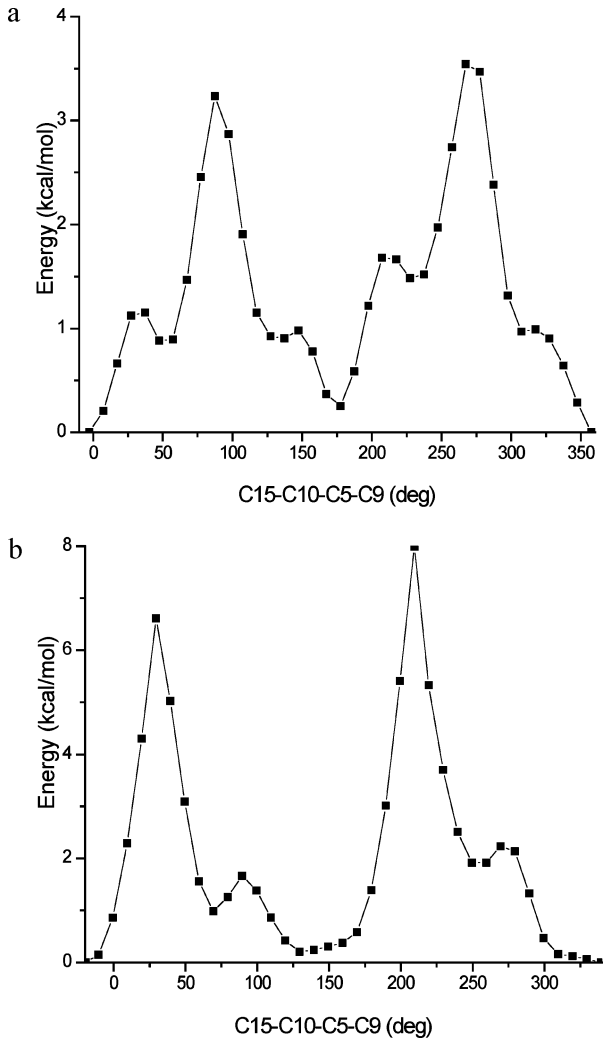

Figure 4. (a) Potential energy of (1*R*,5*S*)-**1b** vs the dihedral angle of C15−C10−C5−C9; (b) potential energy of (1*R*,5*R*,9*S*)-(−)-**10** vs the dihedral angle of C15−C10−C5−C9.

We first varied the dihedral angle of C15−C10−C5−C9 in increments of 10° while relaxing the rest of the structure of **1b**, (1*R*,5*R*,9*S*)-(−)-**10**, (1*R*,5*S*)-(+)-**14**, and (1*R*,5*S*,9*R*)-(+)-**15** to assess the effect of the C9 substituent on the rotational energy barrier of the 5-hydroxyphenyl moiety. The rotation of the 5-hydroxyphenyl of (1*R*,5*S*)-**1b** gives two stable conformers at the dihedral angle of −2.7° and 177.4°, with the former more stable than the latter by 0.25 kcal/mol (Figure 4a); these two rotamers are separated by an energy barrier of 3.2 kcal/mol and 3.5 kcal/mol. The variation of the dihedral angle of C15−C10−C5−C9 of (1*R*,5*R*,9*S*)-(−)-**10** (Figure 4b) from −19.5° to 339.5° also results in two stable rotamers at −19.5° and 129.5° that

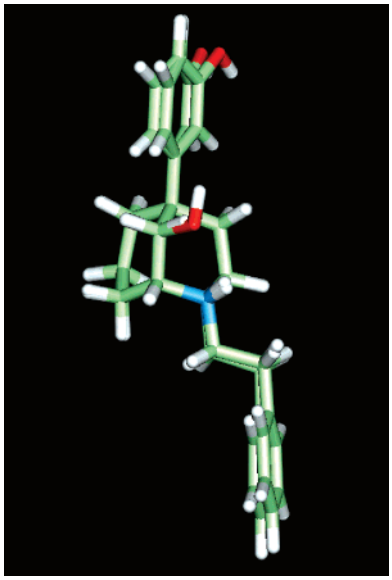

Figure 5. Superposed ab inito energy minimized structures of (1*R*,5*S*)-**1b** and (1*R*,5*R*,9*S*)-(−)-**10**. Atoms represented by colors as follows: white, hydrogen; green, carbon; blue, nitrogen; red, oxygen.

are separated by an energy barrier of 6.6 kcal/mol and 8.0 kcal/mol, depending on the direction of the phenol ring rotation. In terms of thermochemical stability, the rotamer at the dihedral angle of −19.5° is 0.20 kcal/mol more stable than the rotamer at 129.5°. Apparently, the presence of the β-oriented (axial to the piperidine ring) hydroxyl moiety at C9 raises the first rotational energy barrier of (1*R*,5*R*,9*S*)-(−)-**10** by 3.4 kcal/mol, as compared to that of (1*R*,5*S*)-**1b**, resulting from the steric repulsion between the C9-OH and the C11-H (or C15-H) of the phenol (see Figure 1 for numbering). Nonetheless, because of the small energy barrier and comparable energy, the two rotamers of (1*R*,5*R*,9*S*)-(−)-**10** exist at room temperature and undergo a rapid interconversion on a sub-microsecond scale. The rigid fitting of (1*R*,5*S*)-**1b** onto (1*R*,5*R*,9*S*)-(−)-**10** using the nine atoms of the morphan moiety, that is, C1−C9, as a common docking site gives a 0.04 Å root-mean-square deviation (rmsd), suggesting essentially no change in the backbone of the two compounds. Moreover, the spatial orientation of the phenol of (1*R*,5*R*,9*S*)-(−)-**10** at −19.5° is quite comparable to that of (1*R*,5*S*)-**1b** at −2.7°, as depicted in Figure 5. Even the rotation of the dihedral angle, C15−C10−C5−C9, of (1*R*,5*R*,9*S*)-(−)-**10** to match that of (1*R*,5*S*)-**1b** (i.e., from −19.5° to −2.7° and 129.5° to 177.4°) requires only a small energy penalty of ∼0.6 kcal/mol and ∼1.0 kcal/mol, respectively. These small energy differences clearly indicate that all phenolic ring conformations in (1*R*,5*S*)-**1b** are readily accessible by the phenolic ring of (1*R*,5*R*,9*S*)-(−)-**10**, and thus, the difference in the spatial position of the phenolic ring between (1*R*,5*S*)-**1b** and (1*R*,5*R*,9*S*)-(−)-

Table 4. Energetics of the Rotamers Calculated with Density Functional Theory at the B3LYP/6-31G* Level

compound	dihedral angle of C15−C10−C5−C9 (deg) of rotamers			rotational energy barriers of the phenol[b] (kcal/mol)	
(1*R*,5*S*)-**1b**	−2.7	177.4 (0.25)[a]		3.2	3.5
(1*R*,5*R*,9*S*)-(−)-**10**	−19.5	129.5 (0.20)		6.6	8.0
(1*R*,5*S*)-(+)-**14**	−58.1	61.9 (−0.26)	121.9 (−0.22)	8.7	8.3
(1*R*,5*S*,9*R*)-(+)-**15**	53.0	233.0 (0.6)		7.5	7.5

[a] Values in parenthesis represent the relative stability (kcal/mol) with respect to the first rotamer. [b] With respect to the first rotamer.

10 is not responsible for the antagonist or agonist activity. Similar energy barriers and energetics were obtained with the 9-methylene and 9α-methyl substitution as reported in Table 4. If we assume that the μ-opioid receptor did not stabilize a particular rotamer, the quantum chemical studies that we report here suggest that it is unlikely that ex vivo potency or agonist versus antagonist behavior of the 9β-methyl compound[12] could be ascribed to a rotamer; these results do not support the hypothesis that a C9β-methyl moiety in the phenylmorphan could produce sufficient steric hindrance to effect pharmacological activity.

As we previously noted, it is surprising to find C9-substituted 5-phenylmorphans containing an *N*-phenylethyl moiety that are μ-agonists. Although compounds with an *N*-phenylethyl moiety in the morphinan, 6,7-benzomorphan, and 4,5-epoxymorphinan series of analgesics are well-known to display increased antinociceptive potency over the related *N*-methyl compound, all of the *N*-phenylethyl substituted 5-phenylmorphans that have formerly been reported were pure μ-antagonists. There is no rationale, that we are aware of, that satisfactorily relates agonist and antagonist effects to molecular structure in this opioid series.

Agonist Potency. Overlay of (1*R*,5*R*,9*S*)-(−)-10, (1*R*,5*S*)-(+)-14, and (1*R*,5*S*,9*R*)-(+)-15. It is possible to rationalize the high agonist potency of (1*R*,5*R*,9*S*)-(−)-**10** if we hypothesize that the agonist activity of this series of compounds might be correlated with a proton transfer of the charged nitrogen atom via a channeled water molecule(s) to an appropriate amino acid in the μ-opioid receptor. If that occurred, a subsequent conformational change in the receptor induced by the proton transfer might initiate the signaling process that culminates in agonist activity.

The morphan moiety of (1*R*,5*R*,9*S*)-(−)-**10** fits well to the corresponding atoms of the geometry optimized structure of morphine (rmsd <0.14 Å), whereas its enantiomer, (1*S*,5*S*,9*R*)-(+)-**10**, which was found to have 60-fold less affinity for the μ-receptor, does not readily fit. A similar trend is also observed for (1*R*,5*S*)-(+)-**14** and (1*R*,5*S*,9*R*)-(+)-**15**, as shown in Table 1. Among (1*R*,5*R*,9*S*)-(−)-**10**, (1*R*,5*S*)-(+)-**14**, and (1*R*,5*S*,9*R*)-(+)-**15**, the stereochemistry of the morphan is identical except at C9, suggesting that the differences in their binding affinities and pharmacological responses arise from the chemical nature of the hydroxyl, methylene, and methyl substituent as well as from their spatial orientation at C9. To probe this possibility, the geometry optimized structures of (1*R*,5S)-(+)-**14** and (1*R*,5*S*,9*R*)-(+)-**15** were overlaid onto (1*R*,5*R*,9*S*)-(−)-**10** using the morphan atoms as a common docking site as shown in Figure 6a. The rmsd of the fitting of (+)-**14** and (+)-**15** onto (−)-**10** is 0.04 Å and 0.05 Å, respectively. The C9-hydroxyl oxygen, methylene carbon, and methyl carbon are positioned 2.6 Å, 3.4 Å and 3.9 Å, respectively, away from their respective protonated nitrogen. We observed that the C9β-hydroxyl in (1*R*,5*R*,9*S*)-(−)-**10** is especially well-positioned to form a water-mediated H-bond with the protonated nitrogen. Insertion of a water molecule between the C9β-hydroxyl and the nitrogen atom and subsequent geometry optimization (Figure 6b) suggests that a water molecule can be part of a seven-membered ring involved in H-bonding with the OH and the tertiary nitrogen. With the addition of a second water molecule, a short H-bonded water

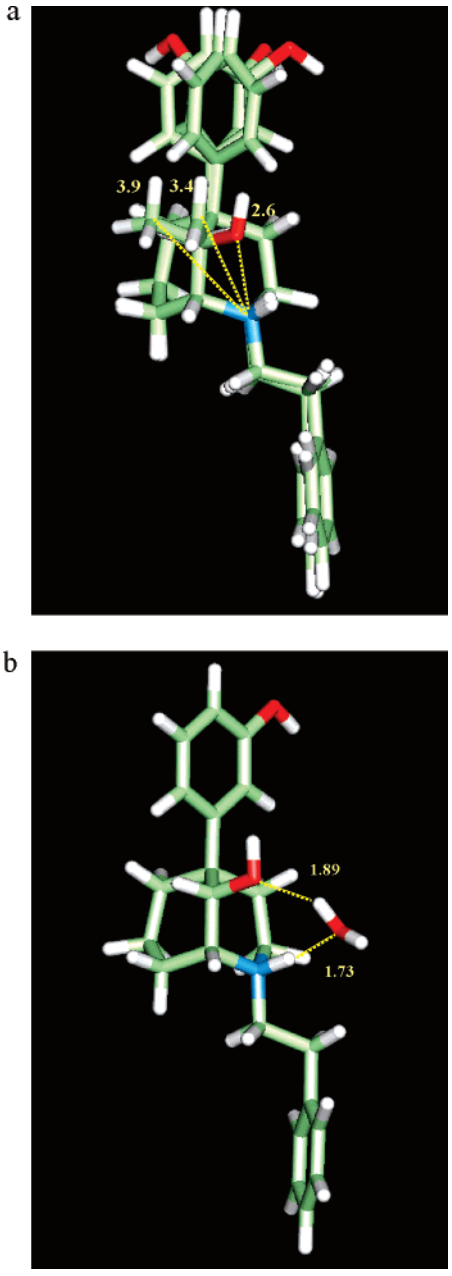

Figure 6. (a) Superposed structures of (1*R*,5*R*,9*S*)-(−)-**10**, (1*R*,5*S*)-(+)-**14**, and (1*R*,5*S*,9*R*)-(+)-**15**. Dotted lines indicate the distance between the heavy atoms of the C9-substituents and the protonated tertiary nitrogen atom. The C9-hydroxyl oxygen in (1*R*,5*R*,9*S*)-(−)-**10**, methylene carbon in (1*R*,5*S*)-(+)-**14**, and methyl carbon in (1*R*,5*S*,9*R*)-(+)-**15** are positioned 2.6 Å, 3.4 Å, and 3.9 Å, respectively, away from the protonated nitrogen. (b) H-bonding interaction of a putative water molecule with the 9β-OH and the protonated tertiary nitrogen of (1*R*,5*R*,9*S*)-(−)-**10**.

chain can form, which in turn effectively polarizes the hydrogen of the tertiary nitrogen. This observation has led us to hypothesize that, in μ-opioid receptors, a putative H-bonded water chain pulls the proton from the protonated tertiary amine and then facilitates a proton hopping along the chain, a process known as a Grotthuss mechanism,[21] to a nearby proton acceptor, possibly Asp, a well-conserved residue among the opioid G-protein coupled receptors (GPCR). Proton transfer via a H-bonded water chain inside proteins is a well-known process.[22] A change in the local protonation state is also known to cause substantial conformational changes in proteins such as cytochrome oxidase,[23] bacteriorhodopsin,[24] and green fluorescent protein.[25] Accordingly, analogous conformational changes in the μ-opioid receptor caused by the proton transfer may provide the signal that induces μ-agonist activity through the opioid receptor.

The possibility that proton transfer influences the agonist activity of an opioid was first raised by Belleau et al.[26] and Kolb and Scheiner.[27] They envisioned a direct proton transfer from the nitrogen atom. While this kind of direct transfer is feasible, structural evidence from recent X-ray diffraction studies support proton transfer via an aligned H-bonded water chain. Examples of proteins with an interior water chain includes bacteriorhodopsin,[28] a GPCR, cytochrome-c oxidase,[23] green fluorescent protein,[25] and gramicidin.[29] In particular, the X-ray structure of bacteriorhodopsin of the N′ state[28] has shown a H-bonded water chain connecting the proton donor Asp-85 to the Schiff base nitrogen of retinal, and quantum chemical dynamics simulations have indicated that this water chain facilitates the proton hopping during the transition from the late M to the N state.[30] In addition, the stability induced by H-bonding through a water molecule(s), as shown in Figure 6b, lends further support to the premise that the agonist activity of (1*R*,5*R*,9*S*)-(−)-**10** is enhanced because of the presence of the 9-hydroxyl moiety in (−)-**10**, which may promote the alignment of water molecule(s).

The hydrophobic methylene and methyl substituents at C9 may also aid the alignment of water molecule(s) by restricting the movement of putative water molecules at the opioid binding site. This proposition is supported by recent computer simulations that have shown that the confined hydrophobic environment of the interior of both bacteriorhodopsin[30] and carbon nanotubes[31,32] favors the alignment of a H-bonded water chain. The putative water chain induced by the C9-methylene of (1*R*,5*S*)-(+)-**14** and the C9-methyl of (1*R*,5*S*,9*R*)-(+)-**15**, however, may not be quite as well aligned as in (1*R*,5*R*,9*S*)-(−)-**10**, making the proton transfer somewhat less favorable because these C9 moieties are spatially further from the *N*-atom. This may give rise to the more modest agonist behavior of (1*R*,5*S*)-(+)-**14**. The 9α-methyl of (1*R*,5*S*,9*R*)-(+)-**15** is even further from the tertiary nitrogen (3.9 Å vs 2.6 Å and 3.4 Å for the related C9β-hydroxy and the methylene compounds, respectively) and, thus, a weaker μ-agonist than the other two compounds in the [^{35}S]GTP-γ-S assay and in vivo (data not shown). Nevertheless, the 9α-methyl still seems to be fairly effective in aligning water molecules and the compound has some activity as an agonist, unlike **1b** that was a pure antagonist ex vivo.[4,9] The distance of these moieties from the nitrogen atom appear, at least in this limited sample of three compounds, to be compatible with the alignment of the water chain and, perhaps, with their in vivo activity.

Conclusion

The synthesis of the enantiomers of the various C9-substituted phenylmorphans yielded compounds with very high affinity for the μ-opioid receptor, and two of these produced extremely potent antinociceptive effects in standard assays of nociception. One of them, (1*R*,5*S*)-(+)-**14**, exhibited a profile consistent with a mixed-acting μ-agonist and a μ-,δ- and κ-antagonist ex vivo. That compound, however, was found to have morphine-like actions in the single dose suppression assay in monkeys and, in an antinociceptive assay, showed typical signs of morphine-like agonist activity (Straub tail and stereotypic circling behavior). It did not show any antagonist activity in vivo.

Quantum chemical calculations did not provide any assurance that the change in types of activities (agonist vs antagonist) could be ascribed to the presence or absence of steric hindrance caused by a C9-substituent. The question of what distinguishes opioid agonists and antagonists at the molecular level remains intriguing. Although agonist activity for an *N*-phenylethyl-substituted phenylmorphan was unexpected, our hypothesis of the facilitation of aligned water molecules by a properly positioned 9-hydroxy substituent and a protonated nitrogen atom enabling water-assisted proton transfer from the ligand to an amino acid in the μ-receptors' binding pocket, provides a possible explanation of the remarkable μ-opioid agonist potency found for the 9β-hydroxy compound. This hypothesis is being further examined, and the results that are obtained will be reported in the future.

Experimental Section

The experimental procedures are written for the (1*S*,5*S*)-enantiomers. The (1*R*,5*R*)-enantiomers were prepared following the same conditions. All reactions were performed in oven-dried glassware under an argon atmosphere and magnetically stirred, unless otherwise noted. All melting points were determined on a Thomas-Hoover melting point apparatus and are uncorrected. Radial preparative layer chromatography (radial PLC) was performed on a Chromatotron (Harrison Associates, Palo Alto, CA) using glass plates coated with 1, 2, or 4 mm layers of Kieselgel 60 PF254 containing gypsum. Proton (^{1}H NMR in $CDCl_3$, unless otherwise stated, with TMS at δ 0.0 ppm) and carbon (^{13}C NMR with $CDCl_3$ at δ 77.23 ppm) spectra were recorded on a Varian XL-300 instrument at 300 MHz for ^{1}H NMR and 75 MHz for ^{13}C NMR. A temperature of 55 °C was used when needed for rotamer coalescence. Mass spectra (ES) and high-resolution mass spectra (HRMS) were obtained using a JEOL SX102. Thin layer chromatography (TLC) was performed on 250 mm Analtech GHLF silica gel plates using various gradients of $CHCl_3$/MeOH containing 1% NH_4OH or gradients of ethyl acetate/*n*-hexanes. Visualization was accomplished under UV or by staining in an iodine chamber. Elemental analyses were performed by Atlantic Microlabs, Inc., Norcross, GA.

Quantum Chemical Methods. Geometry optimization and energetic calculations for all the compounds in Table 1 have been conducted in the gaseous phase with the density functional theory at the level of B3LYP/6-31G*.[33] No thermal energy and solvents effects were taken into account in calculating rotational energy barriers. Superposition of these geometry-optimized structures was carried out using the rigid-fit of Quanta 2000 (Accelrys). This fit method minimizes the root-mean-square deviation between reference and working compounds as a function of both translational and rotational (or orientational) degrees of freedom.

Antinociceptive (Hot Plate, Tail-Flick, Phenylquinone) Assays in Mice and Single-Dose Suppression Assay in Monkeys. These assays were run as previously noted.[34]

Warm Water Tail-Flick Test. Antinociception was assessed at 55 °C. The latency to the first sign of a rapid tail-flick was taken as the behavioral endpoint. Each mouse was first tested for baseline latency by immersing its tail in the water and recording the time to response. Mice not responding within 5 s were excluded from further testing. Mice were then administered the test compound and tested for antinociception at 10, 20, 30, 45, 60, 90, 120, and

180 min postinjection. A cutoff of 10 s was used to avoid tissue damage. Antinociception was calculated by the following formula: % antinociception = 100 × (test latency-control latency)/(10-control latency). Dose−response lines were constructed at times of peak agonist effect and analyzed by linear regression using FlashCalc software (Dr. Michael Ossipov, University of Arizona, Tucson, AZ). All A_{50} values (95% confidence limits) shown are calculated from the linear portion of the dose−response curve. A minimum of three doses/curve and 10 mice/dose were used.

Binding and Efficacy Assays. Cell Culture and Membrane Preparation. The recombinant CHO cells (hMOR-CHO, hDOR-CHO, and hKOR-CHO) were produced by stable transfection with the respective human opioid receptor cDNA and were provided by Dr. Larry Toll (SRI International, CA). The cells were grown on plastic flasks in DMEM (100%; hDOR-CHO and hKOR-CHO) or DMEM/F-12 (50%/50%) medium (hMOR-CHO) containing 10% FBS and G-418 (0.10−0.2 mg/mL) under 95% air/5% CO_2 at 37 °C. Cell monolayers were harvested and frozen at −80 °C.

[^{35}S]GTP-γ-S Binding Assays. On the day of the assay, cells were thawed on ice for 15 min and homogenized using a polytron in 50 mM Tris-HCl, pH 7.4, containing 4 μg/mL leupeptin, 2 μg/mL chymostatin, 10 μg/mL bestatin, and 100 μg/mL bacitracin. The homogenate was centrifuged at 30 000 × *g* for 10 min at 4 °C, and the supernatant was discarded. The membrane pellets were resuspended in binding buffer and were used for [^{35}S]GTP-γ-S binding assays. [^{35}S]GTP-γ-S binding was determined as described previously.[35] Briefly, test tubes received the following additions: 50 μL buffer A (50 mM Tris-HCl, pH 7.4, containing 100 mM NaCl, 10 mM $MgCl_2$, 1 mM EDTA), 50 μL GDP in buffer A/0.1% BSA (final concentration = 10 μM), 50 μL drug in buffer A/0.1% BSA, 50 μL [^{35}S]GTP-γ-S in buffer A/0.1% BSA (final concentration = 50 pM), and 300 μL of cell membranes (50 μg of protein) in buffer B. The final concentrations of reagents in the [^{35}S]GTP-γ-S binding assays were: 50 mM Tris-HCl, pH 7.4, containing 100 mM NaCl, 10 mM $MgCl_2$, 1 mM EDTA, 1 mM DTT, 10 μM GDP, and 0.1% BSA. Incubations proceeded for 3 h at 25 °C. Nonspecific binding was determined using GTP-γ-S (40 μM). Bound and free [^{35}S]-GTP-γ-S were separated by vacuum filtration through GF/B filters. The filters were punched into 24-well plates to which was added 0.6 mL LSC-cocktail (Cytoscint). Samples were counted, after an overnight extraction, in a Trilux liquid scintillation counter at 27% efficiency.

Opioid Binding Assays. [^{125}I]IOXY (6β-iodo-3,14-dihydroxy-17-cyclopropylmethyl-4,5α-epoxymorphinan; SA = 2200 Ci/mmol) was used to label μ-, δ-, and κ-binding sites. On the day of the assay, cell pellets were thawed on ice for 15 min then homogenized with a polytron in 10 mL/pellet of ice-cold 10 mM Tris-HCl, pH 7.4. Membranes were then centrifuged at 30 000 × *g* for 10 min, resuspended in 10 mL/pellet ice-cold 10 mM Tris-HCl, pH 7.4, and again centrifuged 30 000 × *g* for 10 min. Membranes were then resuspended in 25 °C 50 mM Tris-HCl, pH 7.4 (∼100 mL/pellet hMOR-CHO, 50 mL/pellet hDOR-CHO and 120 mL/pellet/hKOR-CHO). All assays took place in 50 mM Tris-HCl, pH 7.4, with a protease inhibitor cocktail [bacitracin (100 μg/mL), bestatin (10 μg/mL), leupeptin (4 μg/mL), and chymostatin (2 μg/mL)], in a final assay volume of 1.0 mL. Nonspecific binding was determined using 10 μM naloxone. Triplicate samples were filtered with Brandell Cell Harvesters (Biomedical Research & Development, Inc., Gaithersburg, MD) over Whatman GF/B filters after a 2 h incubation at 25 °C. The filters were punched into 12 × 75 mm glass test tubes and counted in a Micromedic gamma counter at 80% efficiency. Opioid binding assays had ∼30 μg protein per assay tube. Inhibition curves were generated by displacing a single concentration of radioligand by 10 concentrations of drug.

Data Analysis and Statistics. For [^{35}S]GTP-γ-S binding experiments, the percent stimulation of [^{35}S]GTP-γ-S binding was calculated according to the following formula: $(S - B)/B \times 100$, where B is the basal level of [^{35}S]GTP-γ-S binding and S is the stimulated level of [^{35}S]GTP-γ-S binding.[36] EC_{50} values (the concentration that produces fifty percent maximal stimulation of [^{35}S]GTP-γ-S binding) and E_{max} (% of maximal stimulation in the [^{35}S]-GTP-γ-S binding) were determined using either the program MLAB-PC (Civilized Software, Bethesda, MD) or KaleidaGraph (version 3.6.4, Synergy Software, Reading, PA). For functional K_i determinations, except where otherwise indicated, we determined the ability of test agents to inhibit DAMGO (1 μM)-, SNC80 (500 nM)- or (−)-U50,488 (500 nM)-stimulated [^{35}S]-GTP-γ-S binding, using the appropriate cell line. The data of at least three experiments (10 points each) were pooled, and the data were fit to the two-parameter logistic equation for the best-fit estimates of the IC_{50} and N values: $Y = 100/(1 + ([\text{INHIBITOR}]/IC_{50})^N)$, where Y is the percent of control value. The functional K_i values were then calculated from the IC_{50} values according to the equation: $K_i = IC_{50}/(1 + [D]/ED_{50}(D))$, where D is the concentration of stimulation agent and $ED_{50}(D)$ is the ED_{50} of that agent for stimulating [^{35}S]-GTP-γ-S binding. For opioid binding experiments, the data were fit to the two-parameter logistic equation for the best-fit estimates of the IC_{50} and N values.

Sources. [^{35}S]GTP-γ-S (SA = 1250 Ci/mmol) was obtained from DuPont NEN (Boston, MA). Various opioid peptides were provided by Multiple Peptide System via the Research Technology Branch, NIDA. [^{125}I]IOXY was prepared as described[37,38] using precursor (3-acetoxy-6α-[[(trifluoromethyl)sulfonyl]oxy]-l4-hydroxy-17-(cyclopropylmethyl)-4,5α-epoxymorphinan) synthesized in the laboratory of Dr. Thomas Prisinzano (University of Iowa, Iowa City, IA). The sources of other agents are published.[36]

Optical Resolution of (±)-5-(3-Methoxyphenyl)-2-methyl-9-oxo-2-azabicyclo[3.3.1]nonane ((±)-2). The racemate (15.85 g, (±)-**2**) was diluted in 100 mL of 60% acetone/40% methanol and l-tartaric acid (9.15 g) was dissolved in 75 mL of 60% acetone/40% methanol. The optimal target concentration of the salt was 1 g/7 mL. Both solutions were heated to reflux prior to mixing. The l-tartaric acid solution was quickly added to the base, and the resulting mixture was vigorously mixed. Snow flake-like crystals appeared almost instantaneously. After cooling, the solid was filtered (10.43 g, 41.7%), and a small portion was free-based and analyzed by NMR with (*R*)-(−)-1-phenyl-2,2,2-trifluoroethanol as chiral shift reagent (ee > 85%).[13] The salt was recrystallized from 84 mL of 90% methanol/water to yield 5.26 g (33%) of enantiomerically pure (1*S*,5*S*)-(−)-**2** after free-basing (>99% by NMR): $[\alpha]^{20}_D$ −34.5° (*c* 1.34, $CHCl_3$). The initial filtrate and mother liquors were recovered, evaporated, and free-based (9.23 g, 58%). The absolute stereochemistry of (1*S*,5*S*)-(−)-**2** was established by X-ray analysis of the L-tartrate salt. The residual material from the preparation of the levo enantiomer, which was enriched with (1*R*,5*R*)-(+)-**2**, was diluted in 61 mL of 60% acetone/40% methanol. D-Tartaric acid (5.33 g) was dissolved in 40 mL of 60% acetone/40% methanol. Both solutions were heated to reflux prior to mixing. The D-tartaric acid solution was quickly added to the base, and the resulting mixture was vigorously mixed. Snow flake-like crystals appeared almost instantaneously. After cooling, the solid was filtered (12.2 g, 49%, ee > 70%). After evaporation, the filtrate was worked up to obtain an additional 2.19 g (9%). The salt was recrystallized from 90% methanol/10% water (1 g/8 mL) to obtain enantiomerically pure (1*R*,5*R*)-(+)-**2**: $[\alpha]^{20}_D$ +35.5° (*c* 1.2, $CHCl_3$) after conversion to the free-base.

(1*S*,5*S*)-(−)-Ethyl-5-(3-methoxyphenyl)-9-oxo-2-azabicyclo-[3.3.1]nonane-2-carboxylate, (1*S*,5*S*)-(−)-3). The free-base oil, (1*S*,5*S*)-(−)-**2** (8.72 g, 33.6 mmol), was diluted in 67 mL of anhydrous dichloroethane. To the reaction mixture was added K_2CO_3 (2.21 g, 168 mmol) followed by ethylchloroformate (16.05 mL, 168 mmol). The resulting mixture was refluxed overnight. After that time, some remaining starting material was present and more K_2CO_3 (882 mg, 67.2 mmol) and ethylchloroformate (3.21 mL, 33.6 mmol) were added. The reaction was refluxed for an additional 7 h. Water was then added, and the basicity was adjusted to pH 9 with 28% NH_4OH. The aqueous layer was extracted with $CHCl_3$, and the combined organic extracts were washed with brine and dried over Na_2SO_4. The crude mixture was evaporated in vacuo and purified by flash chromatography (silica gel, 2% MeOH/CH_2Cl_2) to afford (1*S*,5*S*)-(−)-**3** as a white solid (9.32 g, 87%) and some recovered starting material (820 mg, 9%). Mp 92−93 °C; ^{1}H

NMR (55 °C) δ 7.29−7.23 (m, 1H), 6.81−6.78 (m, 3H), 4.39 (broad s, 1H), 4.19 (q, 3H, J = 7.2 Hz), 3.79 (s, 3H), 3.30 (ddd, 1H, J = 5.4, 10.5 and 13.8 Hz), 2.6 (broad s, 1H), 2.51 (ddd, 1H, J = 5.6, 10.5 and 14.3 Hz), 2.39−2.31 (m, 2H), 2.26−2.15 (m, 2H), 1.86−1.71 (m, 2H), 1.28 (t, 3H, J = 7.2 Hz); ^{13}C NMR (55 °C) δ 211.1, 159.8, 145.7, 129.3, 119.7, 114.0, 111.9, 63.6, 61.8, 55.5, 53.2, 42.0, 41.3, 38.6, 18.2, 14.9; HRMS (ES^+) calcd for $C_{18}H_{23}NO_4$ $(M + H)^+$, 318.1705; found, 318.1692. $[\alpha]^{20}_D$ −40.6° (*c* 1.25, $CHCl_3$). Anal. ($C_{18}H_{23}NO_4$): C, H, N. For (1*R*,5*R*)-(+)-**3**: $[\alpha]^{20}_D$ +40.4° (*c* 1.12, $CHCl_3$).

(1*S*,5*S*)-(+)-5-(3-Methoxyphenyl)-9-oxo-2-azabicyclo[3.3.1]-nonane ((1*S*,5*S*)-(+)-4). The carbamate (1*S*,5*S*)-(−)-**3** (10.17 g, 32.04 mmol) was dissolved in 66 mL of anhydrous dichloroethane. Trimethylsilyliodide (6.81 mL, 48.06 mmol) was added dropwise at room temperature. The resulting reaction mixture was then warmed to 55 °C overnight. An additional 1.6 mL (11.3 mmol) of trimethylsilyliodide was added, and the reaction was further stirred at 55 °C for 3 h. The reaction was quenched with an aqueous solution of sodium thiosulfate and basified with 28% NH_4OH. The aqueous layer was extracted with CH_2Cl_2. The combined organic extracts were washed with brine and dried with Na_2SO_4. The crude mixture was evaporated in vacuo and purified by flash chromatography (silica gel, gradient 2% to 5% MeOH/CH_2Cl_2) to afford the product (1*S*,5*S*)-(+)-**4** as an oil (5.63 g, 72%). Some starting material was recovered (800 mg, 8%). ^{1}H NMR δ 7.30−7.25 (m, 1H), 6.86−6.78 (m, 3H), 3.80 (s, 3H), 3.62−3.52 (m, 2H), 3.00 (dt, 1H, J = 6 and 13.8 Hz), 2.54−2.22 (m, 7H), 2.13−2.01 (m, 1H), 1.83−1.74 (m, 1H); ^{13}C NMR δ 216.6, 159.4, 145.9, 129.1, 119.8, 113.9, 111.4, 61.9, 55.4, 53.8, 44.4, 42.1, 40.9, 35.9, 20.0; HRMS (ES^+)) calcd for $C_{15}H_{19}NO_2$ $(M + H)^+$, 246.1494; found, 246.1487; $[\alpha]^{20}_D$ +66.2° (*c* 1.4, $CHCl_3$). For (1*R*,5*R*)-(−)-**4**: $[\alpha]^{20}_D$ −65.4° (*c* 0.86, $CHCl_3$).

(1S,5S)-(−)-5-(3-Methoxyphenyl)-9-oxo-2-phenylethyl-2-azabicyclo[3.3.1]nonane ((1S,5S)-(−)-5). The secondary amine (1*S*,5*S*)-(+)-**4** (4.29 g, 17.5 mmol) was dissolved in anhydrous acetonitrile (60 mL), and K_2CO_3 (7.22 g, 52.5 mmol) and KI (722 mg, 4.35 mmol) were added. 2-Phenylethylbromide (3.62 mL, 26.3 mmol) was then added in one portion, and the resulting reaction mixture was refluxed for 20 h. An additional 1.2 mL of 2-phenylethylbromide was added, and the reaction mixture was refluxed for 4 h to drive the reaction to completion. The solids were filtered, and the resulting filtrate was concentrated in vacuo. The residue was purified by flash chromatography (silica gel, hexanes then gradient CH_2Cl_2 to 2% MeOH/CH_2Cl_2) to afford the (1*S*,5*S*)-(−)-**5** (5.79 g, 95%) as clear crystals: mp 68−70 °C; ^{1}H NMR δ 7.32−7.18 (m, 6H), 6.85−6.77 (m, 3H), 3.80 (s, 3H), 3.35 (t, 1H, J = 3 Hz), 3.28−3.20 (m, 1H), 2.93−2.73 (m, 5H), 2.51−2.35 (m, 4H), 2.22−2.11 (m, 2H), 1.82−1.62 (m, 2H); ^{13}C NMR δ 214.6, 159.4, 146.3, 140.3, 129.1, 128.9, 128.6, 126.3, 119.9, 113.9, 111.4, 69.2, 59.1, 55.4, 53.1, 49.1, 40.8, 39.5, 34.7, 34.4, 19.2; HRMS (ES^+) calcd for $C_{23}H_{27}NO_2$ $(M + H)^+$, 350.2106; found, 350.2120; $[\alpha]^{20}_D$ −29.4° (*c* 1.40, $CHCl_3$,). Anal. ($C_{23}H_{27}NO_2$): C, H, N. For (1*R*,5*R*)-(+)-**5**: $[\alpha]^{20}_D$ +30° (*c* 1.18, $CHCl_3$).

(1*S*,5*S*)-(−)-5-(3-Hydroxyphenyl)-9-oxo-2-phenylethyl-2-azabicyclo[3.3.1]nonane ((1*S*,5*S*)-(−)-6). The methoxyamine (1*S*,5*S*)-(−)-**5** (261 mg, 0.75 mmol) was dissolved in 3.4 mL of glacial acetic acid. A 48% aqueous HBr solution (3.4 mL) was then added, and the reaction was allowed to reflux overnight. The cloudy mixture became clear and yellow upon heating. The mixture was cooled to 0 °C, diluted with H_2O, and basified to pH 10 with a 40% NaOH solution. The aqueous layer was extracted with EtOAc/$CHCl_3$/MeOH (8:1:1). The combined organic extracts were washed with H_2O and brine, dried over Na_2SO_4, and concentrated in vacuo. The crude residue was purified by radial PLC (silica, gradient CH_2Cl_2 to 2% MeOH/CH_2Cl_2) to afford (1*S*,5*S*)-(−)-**6** (188 mg, 75%) as a white foam. The HBr salt of (1*S*,5*S*)-(−)-**6** was formed in Et_2O (1 mL) with 30% HBr in acetic acid (0.12 mL) and recrystallized from absolute ethanol to give a white solid. The analyses were performed on the free base, unless otherwise noted. ^{1}H NMR (free-base, 55 °C) δ 7.32−7.17 (m, 6H), 6.80 (d, 1H, J = 7.5 Hz), 6.73−6.68 (m, 2H), 5.41 (broad s, 1H), 3.36 (t, 1H, J = 3 Hz), 3.29−3.21 (m, 1H), 2.95−2.73 (m, 5H), 2.50−2.33 (m, 4H), 2.25−2.10 (m, 2H), 1.82−1.65 (m, 2H); ^{13}C NMR (55 °C) δ 215.2, 155.6, 146.2, 140.2, 129.3, 128.9, 128.6, 126.3, 119.3, 115.0, 114.0, 68.9, 58.9, 53.0, 49.0, 40.9, 39.4, 34.6, 34.1, 19.3; HRMS (ES^+) calcd for $C_{22}H_{25}NO_2$, 336.1964 $(M + H)^+$; found, 336.1963; $[\alpha]^{20}_D$ −31.9° (*c* 1.115, $CHCl_3$). Anal. ($C_{22}H_{26}BrNO_2$): C, H, N. For (1*R*,5*R*)-(+)-**6**: $[\alpha]^{20}_D$ +32.5° (*c* 0.965, $CHCl_3$). HBr salt: mp 199−202 °C. Anal. ($C_{22}H_{26}BrNO_2 \cdot 0.5H_2O$): C, H, N.

(1*S*,5*S*,9*S*)-(−)-9-Hydroxy-5-(3-methoxyphenyl-2-phenylethyl-2-azabicyclo[3.3.1]nonane ((1*S*,5*S*,9*S*)-(−)-7). Methanol (5 mL) was placed in a flask. To this was added thionyl chloride (0.38 mL, 1.4 mmol, 2 M solution in CH_2Cl_2), and the resulting mixture was stirred for 30 min at room temperature and then cooled to 0 °C. A solution of the phenolic amine (1*S*,5*S*)-(−)-**5** (400 mg, 1.14 mmol) in 2 mL of methanol was then added, and the salt was allowed to form for 30 min at 0 °C. Sodium borohydride (180 mg, 4.8 mmol) was then slowly added, and the resulting mixture was warmed to room temperature. The reaction was quenched with a saturated solution of $NaHCO_3$, and the aqueous layer was extracted with Et_2O. The combined organic extracts were washed with brine and dried over Na_2SO_4. The residue was evaporated and purified by radial PLC (silica, gradient CH_2Cl_2 to 5% MeOH/CH_2Cl_2) to afford the α-alcohol (1*S*,5*S*,9*S*)-(−)-**7** (361 mg, 90%) as a white solid: mp 97−98 °C; ^{1}H NMR δ 7.32−7.17 (m, 6H), 7.06 (d, 1H, J = 7.8 Hz), 7.03 (t, 1H, J = 2.2 Hz), 6.75 (dd, 1H, J = 2.2 and 8 Hz), 4.30 (d, 1H, J = 3.6 Hz), 3.78 (s, 3H), 3.15 (s, 1H), 3.0 (td, 1H, J = 5 and 11.8 Hz), 2.93−2.80 (m, 5H), 2.27−2.06 (m, 2H), 2.00−1.71 (m, 7H); ^{13}C NMR δ 160.0, 149.7, 140.7, 129.7, 128.9, 128.5, 126.2, 118.3, 112.6, 111.2, 73.4, 57.6, 56.6, 55.3, 49.6, 40.8, 39.4, 34.7, 28.9, 22.0, 18.7; HRMS (ES^+) calcd for $C_{23}H_{29}NO_2$, 352.2277 $(M + H)^+$; found, 352.2277; $[\alpha]^{20}_D$ −37.7° (*c* 0.87, $CHCl_3$). Anal. ($C_{23}H_{29}NO_2$): C, H, N. For (1*R*,5*R*,9*R*)-(+)-**7**: $[\alpha]^{20}_D$ +38.4° (*c* 1.47, $CHCl_3$). Anal. ($C_{23}H_{29}NO_2$): C, H, N.

(1*S*,5*S*,9*S*)-(−)-9-Hydroxy-5-(3-hydroxyphenyl-2-phenylethyl-2-azabicyclo[3.3.1]nonane ((1*S*,5*S*,9*S*)-(−)-8). The methoxyphenyl compound (1*S*,5*S*,9*S*)-(−)-**7** (400 mg, 1.14 mmol) was dissolved in 6 mL anhydrous CH_2Cl_2 and cooled to −78 °C. A solution of BBr_3 (1 M, 5.7 mL, 5.7 mmol) was then added dropwise, and the reaction was allowed to warm up slowly overnight. The reaction was cooled back to −78 °C and quenched with H_2O and 28% NH_4-OH. The resulting heterogeneous mixture was warmed to room temperature and vigorously stirred for 1 h, until the CH_2Cl_2 layer was clear. The aqueous layer was extracted with CH_2Cl_2, and the combined organic extracts were washed with brine and dried over Na_2SO_4. The crude was evaporated and purified by radial PLC (silica, 94.5/5/0.5 $CHCl_3$/MeOH/28% NH_4OH) to afford (1*S*,5*S*,9*S*)-(−)-**8** as an off-white foam (367 mg, 96%). The relative stereochemistry of (1*S*,5*S*,9*S*)-(−)-**8** was confirmed by X-ray analysis. ^{1}H NMR δ 7.30−7.25 (m, 2H), 7.22−7.11 (m, 4H), 6.97 (s, 1H), 6.90 (d, 1H, J = 7.5 Hz), 6.68 (dd, 1H, J = 1.6 and 8 Hz), 4.40 (d, 1H, J = 3.6 Hz), 3.20 (s, 1H), 3.00−2.96 (m, 2H), 2.85 (d, 4H, J = 3 Hz), 2.28−2.05 (m, 2H), 1.99−1.75 (m, 6H); ^{13}C NMR δ 156.9, 149.4, 139.9, 129.9, 129.0, 128.7, 126.4, 117.9, 114.5, 113.6, 72.4, 57.3, 27.0, 49.8, 40.3, 38.9, 33.7, 28.6, 21.9, 18.0; HRMS (ES^+) calcd for $C_{22}H_{27}NO_2$, 338.2121 $(M + H)^+$; found, 338.2120; $[\alpha]^{20}_D$ −23.6° (*c* 1.51, $CHCl_3$). Anal. ($C_{22}H_{27}NO_2 \cdot 0.4\ H_2O$): C, H, N. For (1*R*,5*R*,9*R*)-(+)-**8**: $[\alpha]^{20}_D$ +24.1° (*c* 1.7, $CHCl_3$). Anal. ($C_{22}H_{27}NO_2 \cdot 0.3\ H_2O$): C, H, N.

(1*S*,5*S*,9*R*)-(+)-9-Hydroxy-5-(3-methxyphenyl-2-phenylethyl-2-azabicyclo[3.3.1]nonane ((1*S*,5*S*,9*R*)-(+)-9). The 9-keto compound (1*S*,5*S*)-(−)-**5** (200 mg, 0.57 mmol) was dissolved in 5 mL of anhydrous THF and cooled to −78 °C. A solution of lithium triethyl borohydride (superhydride; 1 M, 0.86 mL, 0.86 mmol) was added dropwise, and the resulting mixture was stirred for 45 min at −78 °C. The reaction was quenched with H_2O, and the basicity was adjusted to pH 9 with 28% NH_4OH. The aqueous layer was extracted with Et_2O. The combined organic extracts were washed with brine and dried over Na_2SO_4. The residue was evaporated and purified by radial PLC (silica, gradient CH_2Cl_2 to 2% MeOH/CH_2-Cl_2) to afford the β-alcohol (1*S*,5*S*,9*R*)-(+)-**9** (195 mg, 97%) as a thick oil. ^{1}H NMR δ 7.30−7.17 (m, 6H), 7.00 (d, 1H, J = 8.1 Hz),

6.96−6.94 (m, 1H), 6.72 (dd, 1H, J = 2.1 and 8.1 Hz), 4.05 (s, 1H), 3.79 (s, 3H), 3.50 (broad s, 1H), 3.11−2.91 (m, 2H), 2.88−2.77 (m, 4H), 2.35−2.24 (m, 2H), 2.04 (dd, 1H, J = 5.1 and 13.8 Hz), 1.92−1.84 (m, 2H), 1.69−1.50 (m, 4H); ^{13}C NMR δ 159.8, 151.0, 140.5, 129.3, 128.8, 128.6, 126.3, 118.1, 112.4, 110.6, 71.7, 58.9, 56.4, 55.3, 48.3, 41.1, 40.9, 34.5, 30.0, 25.0, 22.9; HRMS (ES$^+$) calcd for $C_{23}H_{29}NO_2$, 352.2277 (M + H)$^+$; found, 352.2261; $[\alpha]^{20}_D$ +55.5° (*c* 1.26, $CHCl_3$,). For (1*R*,5*R*,9*S*)-(−)-**9**: $[\alpha]^{20}_D$ −55.1° (*c* 1.08, $CHCl_3$).

(1*S*,5*S*,9*R*)-(+)-9-Hydroxy-5-(3-hydroxyphenyl-2-phenylethyl-2-azabicyclo[3.3.1]nonane ((1*S*,5*S*,9*R*)-(+)-10). The procedure was identical to the one performed to obtain the C9α-alcohol (1*S*,5*S*,9*S*)-(−)-**8**. The crude residue was purified by radial PLC (silica, 94.5/5/0.5 $CHCl_3$/MeOH/NH_3) to yield 90% of the β-alcohol (1*S*,5*S*,9*R*)-(+)-**10** as an off-white foam. The HCl salt was formed with ($SOCl_2$/MeOH). ^{1}H NMR δ 7.30−7.25 (m, 3H), 7.20−7.11 (m, 3H), 6.91 (d, 1H), 6.85 (s, 1H), 6.57 (dd, 1H, J = 2.3 and 8.3 Hz), 4.35 (broad s, 1H), 4.06 (d, 1H, J = 3.9 Hz), 3.10−2.75 (m, 7H), 2.33−2.22 (m, 2H), 2.02 (dd, 1H, J = 5 and 13.7 Hz), 1.90−1.83 (m, 3H), 1.67−1.47 (m, 3H); ^{13}C NMR δ 156.3, 150.5, 140.3, 129.4, 128.8, 128.6, 126.3, 117.3, 113.2, 113.0, 71.7, 58.8, 56.4, 48.3, 40.8, 40.7, 34.3, 29.7, 24.8, 22.7; HRMS (ES$^+$) calcd for $C_{22}H_{27}NO_2$, 338.2120 (M + H)$^+$; found, 338.2112; $[\alpha]^{20}_D$ +50.9° (*c* 1.18, $CHCl_3$). (1*S*,5*S*,9*R*)-(+)-**10**·HCl: mp 138−142 °C. Anal. ($C_{22}H_{28}ClNO_2$·0.5H_2O): C, H, N. For (1*R*,5*R*,9*S*)-(−)-**10**: $[\alpha]^{20}_D$ −51.8° (*c* 0.82, $CHCl_3$). Anal. ($C_{22}H_{28}ClNO_2$·0.6H_2O): C, H, N.

(1*S*,5*S*)-(−)-9-Hydroxy-5-(3-hydroxyphenyl-2-phenylethyl-9-trimethylsilylmethyl-2-azabicyclo[3.3.1]nonane ((1*S*,5*S*)-(−)-11). The ketone (1*S*,5*S*)-(−)-**5** (1.5 g 4.3 mmol) was dissolved in 25 mL of anhydrous THF and cooled to 0 °C. An ethereal solution of (trimethylsilylmethy)magnesium chloride (17.2 mL, 17.2 mmol) was added. After 20 min, the ice bath was removed and the mixture was warmed to room temperature over 1 h, and refluxed overnight. The reaction was cooled to 0 °C and quenched with dilute NH_4-OH, $CHCl_3$ was added, and the organic phase was separated. The aqueous phase was filtered to remove the thick magnesium salts and extracted with $CHCl_3$. The combined organic phases were washed with brine, dried over Na_2SO_4, and evaporated under reduced pressure. The residue was purified by radial PLC (silica, gradient hexanes/EtOAc 100% to 90% followed by CH_2Cl_2) to afford the pure compound (1*S*,5*S*)-(−)-**11** as a pale yellow oil (1.73 g, 92%). ^{1}H NMR δ 7.43−7.29 (m, 8H), 6.91−6.88 (m, 1H), 3.94 (s, 3H), 3.23−3.18 (m, 2H), 2.96−2.83 (m, 5H), 2.77−2.66 (m, 2H), 2.12−1.55 (m, 8H), 0.52 (d, 1H, J = 14.7 Hz), 0.00 (s, 9H); ^{13}C NMR δ 159.5, 149.0, 141.2, 129.0, 128.8, 128.5, 126.1, 120.3, 114.7, 110.8, 77.1, 62.0, 57.8, 55.4, 48.7, 45.1, 34.8, 33.4, 24.1, 22.3, 19.4, 0.8; HRMS (ES$^+$) calcd for $C_{27}H_{39}NO_2Si$, 438.2828 (M + H)$^+$; found, 438.2824; $[\alpha]^{20}_D$ −17.0° (*c* 1.575, $CHCl_3$). For (1*R*,5*R*)-(+)-**11**: $[\alpha]^{20}_D$ +17.2° (*c* 1.325, $CHCl_3$).

(1*S*,5*R*)-(−)-5-(3-Methoxyphenyl)-9-methylene-2-phenethyl-2-azabicyclo[3.3.1]nonane ((1*S*,5*R*)-(−)-12). The tertiary alcohol (1*S*,5*S*)-(−)-**11** (1.73 g, 3.96 mmol) was diluted in anhydrous THF. Sodium hydride (632 mg, 15.8 mmol) was added, and the mixture was allowed to reflux overnight. The reaction was cooled to 0 °C and stopped by the addition of H_2O and 28% NH_4OH. The aqueous phase was extracted with CH_2Cl_2, dried over Na_2SO_4, and concentrated in vacuo. The residue was purified by radial PLC (silica, gradient CH_2Cl_2, 5% MeOH/CH_2Cl_2) to afford (1*S*,5*R*)-(−)-**12** as a pale yellow oil in 98% yield (1.34 g, 3.56 mmol). ^{1}H NMR ($CDCl_3$, 300 MHz) δ 7.32−7.20 (m, 6H), 6.98 (d, 1H, J = 8.4 Hz), 6.95−6.94 (m, 1H), 6.76 (dd, 1H, J = 2.4 and 8.4 Hz), 4.83 (s, 1H), 4.20 (s, 1H), 3.81 (s, 3H), 3.43 (m, 1H), 3.11−3.03 (m, 1H), 2.87−2.75 (m, 5H), 2.37−2.28 (m, 1H), 2.24−2.00 (m, 5H), 1.71−1.67 (m, 1H), 1.59−1.48 (m, 1H); ^{13}C NMR ($CDCl_3$, 75 MHz) δ 159.3, 154.3, 150.3, 140.9, 129.0, 128.8, 128.6, 126.2, 120.3, 114.2, 110.7, 108.9, 63.9, 59.2, 55.4, 49.0, 44.2, 39.1, 38.3, 34.8, 32.4, 20.4; HRMS (ES+) calcd for $C_{24}H_{29}NO$, 348.2327 (M + H)$^+$; found, 348.2325; $[\alpha]^{20}_D$ −58.9 (*c* 1.87, $CHCl_3$). For (1*R*,5*S*)-(+)-**12**: $[\alpha]^{20}_D$ +59.5 (*c* 1.20, $CHCl_3$).

Alternate method: The starting ketone (1*S*,5*S*)-(−)-**5** (2 g, 5.7 mmol) was diluted in 30 mL of anhydrous THF and cooled to 0 °C. Tebbe's reagent[18,19] (11.4 mL, 5.7 mmol, 0.5 M solution in toluene) was slowly added. The resulting mixture was stirred at 0 °C for 1 h and then slowly warmed up to room temperature for an additional 2 h. The reaction was cooled to 0 °C and 50 mL of Et_2O was added. The reaction was quenched carefully with 1.8 N NaOH. A very vigorous gas evolution took place and a thick green precipitate formed. Magnesium sulfate was added, and the mixture was allowed to stir an additional 5 min. The solids were filtered and washed with EtOAc. The filtrate was concentrated and purified by flash chromatography (silica, gradient, 1−5% MeOH/1%NH_4OH/$CHCl_3$) to afford the product (1*S*,5*R*)-(−)-**12** in 75% yield (1.48 g) as a pale yellow oil.

(1*S*,5*R*,9*S*)-(−)-5-(3-Methoxyphenyl)-9-methyl-2-phenethyl-2-azabicyclo[3.3.1]nonane ((1*S*,5*R*,9*S*)-(−)-13). The C9-methylene compound (1*S*,5*R*)-(−)-**12** (610 mg, 1.73 mmol) was placed in a Parr shaker vessel along with 9 mL of anhydrous MeOH and platinum oxide (40 mg, 0.17 mmol). The mixture was shaken for 2 h under a 35 psi atmosphere of hydrogen. The mixture was filtered over celite. Concentration of the residue and purification by radial PLC (silica, 2% MeOH/CH_2Cl_2) afforded the product (1*S*,5*R*,9*S*)-(−)-**13** (566 mg, 1.59 mmol) in 93% yield as a pale yellow oil. ^{1}H NMR δ 7.33−7.21 (m, 6H), 7.00 (d, 1H, J = 8 Hz), 6.964−6.959 (m, 1H), 6.74−6.71 (m, 1H), 3.80 (s, 3H), 3.03 (dd, 2H, J = 3.5 and 9.8 Hz), 2.89−2.80 (m, 5H), 2.47−2.45 (m, 1H), 2.25−2.05 (m, 2H), 1.99−1.90 (m, 3H), 1.85−1.75 (m, 2H), 1.59−1.54 (m, 1H), 0.76 (d, 3H, J = 7.2 Hz); ^{13}C NMR δ 159.7, 152.2, 141.0, 129.2, 129.0, 128.6, 126.2, 118.3, 112.3, 110.5, 60.1, 58.3, 58.2, 55.4, 50.3, 41.8, 40.1, 38.5, 34.9, 28.5, 22.2, 18.7, 14.4; HRMS (ES$^+$) calcd for $C_{24}H_{31}NO$, 350.2484 (M + H)$^+$; found, 350.2474; $[\alpha]^{20}_D$ −38.4° (*c* 1.43, $CHCl_3$). For (1*R*,5*S*,9*R*)-(+)-**13**: $[\alpha]^{20}_D$ +39.5° (*c* 1.31, $CHCl_3$).

(1*S*,5*R*)-(−)-5-(3-Hydroxyphenyl)-9-methylene-2-phenethyl-2-azabicyclo[3.3.1]nonane ((1*S*,5*R*)-(−)-14). The methoxyphenyl compound (1*S*,5*R*)-(−)-**12** was submitted to the same reaction conditions that were used to obtain the phenolic alcohol (1*S*,5*S*,9*S*)-(−)-**8**. Purification of the crude residue by radial PLC (silica, gradient 2% to 5% MeOH/CH_2Cl_2) gave the free phenol in 96% yield. It was converted to the oxalate salt: light tan solid; mp 113−115 °C. Oxalate: ^{1}H NMR (CD_3OD) δ 7.40−7.29 (m, 5H), 7.21 (t, 1H, J = 8 Hz), 6.89−6.84 (m, 2H), 6.74−6.71 (m, 1H), 5.28 (s, 1H), 4.66 (s, 1H), 4.31 (s, 1H), 3.83 (m, 1H), 3.51−3.45 (m, 3H), 3.16−3.10 (m, 2H), 2.57 (m, 1H), 2.42−2.38 (m, 1H), 2.24−1.95 (m, 6H); ^{13}C NMR δ 156.1, 152.9, 149.7, 140.3, 129.1, 128.94, 128.90, 128.6, 126.3, 119.3, 115.4, 113.7, 109.6, 63.4, 58.6, 48.7, 43.9, 39.0, 37.5, 34.2, 31.0, 21.0; α_D −27.6° (*c* 0.79, MeOH). Anal. ($C_{25}H_{29}NO_5$·0.1H_2O): C, H, N. HRMS of the free base (ES$^+$) calcd for $C_{23}H_{28}NO$, 334.2171 (M + H)$^+$; found, 334.2171. For (1*R*,5*S*)-(+)-**14** oxalate: $[\alpha]^{20}_D$ +26.5° (*c* 0.79, MeOH). Anal. ($C_{25}H_{29}NO_5$·0.1H_2O): C, H, N.

(1*S*,5*R*,9*S*)-(−)-5-(3-Hydroxyphenyl)-9-methyl-2-phenethyl-2-azabicyclo[3.3.1]nonane ((1*S*,5*R*,9*S*)-(−)-15). The methoxyphenyl compound (1*S*,5*R*,9*S*)-(−)-**13** was submitted to the same reaction conditions used to obtain the phenol (1*S*,5*S*,9*S*)-(−)-**8**. After purification by radial PLC (silica, gradient 2% to 5% MeOH/CH_2Cl_2), the product (1*S*,5*R*,9*S*)-(−)-**15** was isolated in 72% yield as a light tan solid, mp 173−174 °C. ^{1}H NMR δ 7.33−7.15 (m, 6H), 6.96 (d, 1H, J = 7.8 Hz), 6.87 (s, 1H), 6.66 (dd, 1H, J = 2.4 and 7.8 Hz), 3.06−3.01 (m, 2H), 2.92−2.79 (m, 5H), 2.48 (s, 1H), 2.25−2.05 (m, 2H), 1.95−1.74 (m, 5H), 1.59−1.57 (m, 2H); ^{13}C NMR δ 156.9, 151.3, 139.8, 129.4, 128.9, 128.7, 126.4, 117.4, 113.8, 113.7, 58.3, 58.7, 50.3, 40.6, 39.0, 38.0, 33.5, 28.0, 21.8, 18.1, 14.1; HRMS (ES$^+$) calcd for $C_{23}H_{30}NO$, 336.2327 (M + H)$^+$; found, 336.2326; $[\alpha]^{20}_D$ −36.1° (*c* 0.79, $CHCl_3$). Anal. ($C_{23}H_{29}NO$·0.1H_2O): C, H, N. For (1*R*,5*S*,9*R*)-(+)-**15**: $[\alpha]^{20}_D$ +35.9° (c 0.79, $CHCl_3$). Anal. ($C_{23}H_{29}NO$·0.1H_2O): C, H, N. The relative stereochemistry of (1*R*,5*S*,9*R*)-(+)-**15** was confirmed by X-ray analysis.

X-ray Crystal Structure of (1*S*,5*S*)-(−)-2, (1*S*,5*S*,9*S*)-(−)-8, and (1*R*,5*S*,9*R*)-(+)-15. Single-crystal X-ray diffraction data were

collected at 93 °K using MoK radiation and a Bruker SMART 1000 CCD area detector. Crystals were prepared for data collection by coating with high viscosity microscope oil (Paratone-N, Hampton Research). Corrections were applied for Lorentz, polarization, and absorption effects. The structures were solved by direct methods and refined by full-matrix least squares on F^2 values using the programs found in the SHELXTL suite.[39] Parameters refined included atomic coordinates and anisotropic thermal parameters for all nonhydrogen atoms. Hydrogen atoms on carbons were included using a riding model (coordinate shifts of C applied to H atoms), with the C−H distance set at 0.96 Å. The absolute configuration was set based on the known configuration of the starting materials for the synthesis or a cocrystallized chiral salt.

(1*S*,5*S*)-(−)-2: An oil-coated 0.52 × 0.29 × 0.19 mm^3 crystal of (1*S*,5*S*)-(−)-**2** was mounted on a glass rod and transferred immediately to the cold stream (−180 °C) on the diffractometer. The crystal was orthorhombic in space group $P2_1$, with unit cell dimensions $a = 6.0987(19)$ Å, $b = 6.907(2)$ Å, and $c = 22.526(7)$ Å. Data were 95.6% complete to 27.98° θ (approximately 0.75 Å). The asymmetric unit contains one molecule plus one molecule of L-tartaric acid.

(1*S*,5*S*,9*S*)-(−)-8: An oil-coated 0.68 × 0.28 × 0.19 mm^3 crystal of (1*S*,5*S*,9*S*)-(−)-**8** was mounted on a glass rod and transferred immediately to the cold stream (−180 °C) on the diffractometer. The crystal was orthorhombic in space group $P2_12_12_1$ with unit cell dimensions $a = 7.1948(9)$ Å, $b = 10.3050(14)$ Å, and $c = 24.896(4)$ Å. Data were 97.0% complete to 28.35° θ (approximately 0.75 Å). The asymmetric unit contains a single molecule.

(1*R*,5*S*,9*R*)-(+)-15: An oil-coated 0.48 × 0.21 × 0.16 mm^3 crystal of (1*R*,5*S*,9*R*)-(+)-**15** was mounted on a glass rod and transferred immediately to the cold stream (−180 °C) on the diffractometer. The crystal was orthorhombic in space group $P2_12_12_1$ with unit cell dimensions $a = 8.3455(13)$ Å, $b = 10.9441(18)$ Å, and $c = 19.225(3)$ Å. Data were 94.3% complete to 28.33° θ (approximately 0.75 Å). The asymmetric unit contains a single molecule.

Acknowledgment. The research of the Drug Design and Synthesis section, CBRB, NIDA, was supported by the NIH Intramural Research Programs of the National Institute of Diabetes and Digestive and Kidney Diseases and the National Institute on Drug Abuse, and the latter supported the research of the Clinical Psychopharmacology section. Y.S.L. thanks Dr. Sergio Hassan for many helpful discussions. The quantum chemical study utilized the high-performance computer capabilities of the Helix Systems at the NIH (http://helix.nih.gov) and the PC/LINUX clusters at the Center for Molecular Modeling of the NIH (http://cit.nih.gov), and this research was supported by the NIH Intramural Research Program through the Center for Information Technology. The authors also acknowledge the expert technical assistance of Mario Ayestas (NIDA). We thank Dr. John Lloyd (NIDDK) for the mass spectral data. Some of the pharmacological data were obtained under the auspices of the Drug Evaluation Committee, College on Problems of Drug Dependence. Dr. A. Coop is the recipient of an independent scientist award from NIDA DA K02-19634.

Note Added after ASAP Publication. This manuscript was released ASAP on July 11, 2007, with some citations of ref 12 that should be absent from the second paragraph of the first page, from the first and second paragraphs of Quantum Chemistry, and from the second paragraph of Conclusion. The correct version was posted on August 2, 2007.

Supporting Information Available: Atomic coordinates for (1*S*,5*S*)-(−)-**2**, (1*S*,5*S*,9*S*)-(−)-**8**, and (1*R*,5*S*,9*R*)-(+)-**15** have been deposited with the Cambridge Crystallographic Data Centre (deposition numbers 625527, 625528, 625529, respectively). Copies of the data can be obtained, free of charge, on application to CCDC, 12 Union Road, Cambridge, CB2 1EZ, U.K. [fax: +44(0)-1223−336033; e-mail: deposit@ccdc.cam.ac.uk]. This material is available free of charge via the Internet at http://pubs.acs.org.

References

(1) May, E. L.; Murphy, J. G. Structures Related to Morphine. IV. *m*-Substituted Phenylcyclohexane Derivatives. *J. Org. Chem.* **1955**, *20*, 1197−1201.
(2) Linders, J. T. M.; Flippen-Anderson, J. L.; George, C. F.; Rice, K. C. An Expedient Synthesis of 9-Keto-2-methyl-5-(dimethoxyphenyl)-morphans. *Tetrahedron Lett.* **1999**, *40*, 3905−3908.
(3) Adah, S. A.; Jacobson, A. E.; Rice, K. C.; Dersch, C. M.; Horel, R.; Rothman, R. B. Development of Analogs of *N*-Phenethylphenylmorphan as Potential Narcotic Antagonists. *Abstracts of Papers of the American Chemical Society* **2000**, *220*, U578−U578.
(4) Hashimoto, A.; Coop, A.; Rothman, R. B.; Dersch, C.; Xu, H.; Horel, R.; George, C.; Jacobson, A. E.; Rice, K. C. Synthesis and Pharmacology of Optically Pure *N*-Substituted Phenylmorphans as Opioid Receptor Antagonists. In *Problems of Drug Dependence, 1999*; Harris, L. S., Ed.; National Institute on Drug Abuse Research Monograph 180; NIH Publication No. 00-4737; National Institutes of Health: Washington DC, 2000; p 250.
(5) Thomas, J. B.; Gigstad, K. M.; Fix, S. E.; Burgess, J. P.; Cooper, J. B.; Mascarella, S. W.; Cantrell, B. E.; Zimmerman, D. M.; Carroll, F. I. A Stereoselective Synthetic Approach to *N*-Alkyl-4β-methyl-5-phenylmorphans. *Tetrahedron Lett.* **1999**, *40*, 403−406.
(6) Linders, J. T. M.; Mirsadeghi, S.; Flippen-Anderson, J. L.; George, C.; Jacobson, A. E.; Rice, K. C. Probes for Narcotic Receptor Mediated Phenomena. Part 30. Synthesis of *rac*-(3*R*,6a*S*,11a*R*)-2-Methyl-1,3,4,5,6,11a-hexahydro-2*H*-3,6a-methanobenzofuro[2,3-c]azocin-8-ol, an Epoxy Isomer of 5-Phenylmorphan. *Helv. Chim. Acta* **2003**, *86*, 484−493.
(7) Carroll, F. I.; Zhang, L.; Mascarella, S. W.; Navarro, H. A.; Rothman, R. B.; Cantrell, B. E.; Zimmerman, D. M.; Thomas, J. B. Discovery of the First *N*-Substituted 4β-Methyl-5-(3-hydroxyphenyl)morphan to Possess Highly Potent and Selective Opioid δ Receptor Antagonist Activity. *J. Med. Chem.* **2004**, *47*, 281−284.
(8) Kim, I. J.; Dersch, C. M.; Rothman, R. B.; Jacobson, A. E.; Rice, K. C. A Critical Structural Determinant of Opioid Receptor Interaction with Phenolic 5-Phenylmorphans. *Bioorg. Med. Chem.* **2004**, *12*, 4543−4550.
(9) Hashimoto, A.; Jacobson, A. E.; Rothman, R. B.; Dersch, C. M.; George, C.; Flippen-Anderson, J. L.; Rice, K. C. Probes for Narcotic Receptor Mediated Phenomena. Part 28: New Opioid Antagonists from Enantiomeric Analogues of 5-(3-Hydroxyphenyl)-*N*-phenylethylmorphan. *Bioorg. Med. Chem.* **2002**, *10*, 3319−3329.
(10) Cheng, K.; Kim, I.-J.; Lee, M. J.; Dersch, C. M.; Rothman, R. B.; Jacobson, A. E.; Rice, K. C. Opioid Ligands with Mixed Properties from Substituted Enantiomeric *N*-Phenethyl-5-phenylmorphans. Synthesis of a μ-Agonist, δ-Antagonist, and δ-Inverse Agonists. *Org. Biomol. Chem.* **2007**, 5, 1177−1190.
(11) Schiller, P. W.; Weltrowska, G.; Berezowska, I.; Nguyen, T. M. D.; Wilkes, B. C.; Lemieux, C.; Chung, N. N. TIPP Opioid Peptide Family: Development of δ Antagonists, δ Agonists, and Mixed μ Agonist/δ Antagonists. *Biopolymers* **1999**, *51*, 411−425.
(12) Thomas, J. B.; Zheng, X. L.; Mascarella, S. W.; Rothman, R. B.; Dersch, C. M.; Partilla, J. S.; Flippen-Anderson, J. L.; George, C. F.; Cantrell, B. E.; Zimmerman, D. M.; Carroll, F. I. *N*-Substituted 9β-Methyl-5-(3-hydroxyphenyl)morphans Are Opioid Receptor Pure Antagonists. *J. Med. Chem.* **1998**, *41*, 4143−4149.
(13) Pirkle, W. H.; Burlingame, T. G.; Beare, S. D. Optically Active NMR Solvents VI. The Determination of Optical Purity and Absolute Configuration of Amines. *Terahedron Lett.* **1968**, *9*, 5849−5852.
(14) Lott, R. S.; Chauhan, V. S.; Stammer, C. H. Trimethylsilyl Iodide as a Peptide Deblocking Agent. *J. Chem. Soc., Chem. Commun.* **1979**, 495−496.
(15) Raucher, S.; Bray, B. L.; Lawrence, R. F. Synthesis of (±)-Catharanthine, (+)-Anhydrovinblastine, and (−)-Anhydrovincovaline. *J. Am. Chem. Soc.* **1987**, *109*, 442−446.
(16) Kodato, S.; Linders, J. T. M.; Gu, X.-H.; Yamada, K.; Flippen-Anderson, J. L.; Deschamps, J. R.; Jacobson, A. E.; Rice, K. C. Synthesis of *rac*-(1*R*,4a*R*,9a*R*)-2-Methyl-1,3,4,9a-tetrahydro-2*H*-1,-4a-propanobenzofuro[2.3-c]pyridin-6-ol. An Unusual Double Rearrangement Leading to the *ortho*- and *para*-f Oxide-Bridged Phenylmorphan Isomers. *Org. Biomol. Chem.* **2004**, *2*, 330−336.
(17) Rice, K. C. A Rapid, High-Yield Conversion of Codeine to Morphine. *J. Med. Chem.* **1977**, *20*, 164−165.
(18) Schwarz, J. B.; Meyers, A. Synthesis of Vicinal Stereogenic Tertiary and Quaternary Centers Using Chiral Bicyclic Lactams and Diastereoselective Protonation. Asymmetric Synthesis of (+)-Laurene. *J. Org. Chem.* **1995**, *60*, 6511−6514.

(19) Jung, M. E.; Pontillo, J. Synthetic Approach to Potential Precursors of Sclerophytin A. *Tetrahedron* **2003**, *59*, 2729−2736.
(20) Clive, D. L. J.; Sun, S. Synthesis of the Racemic Tetracyclic Core of CP-225,917−A Model Compound Lacking The Sidearms of the Natural Product. *Terahedron Lett.* **2001**, *42*, 6267−6270.
(21) de Grotthuss, C. J. T. Sur La Décomposition De L'eau Et Des Corps Qu'elle Tient En Dissolution À L'aide De L'électricité Galvanique. *Ann. Chim.* **1806**, *LVIII*, 54−74.
(22) Decoursey, T. E. Voltage-Gated Proton Channels and Other Proton Transfer Pathways. *Physiol. Rev.* **2003**, *83*, 475−579.
(23) Wikstrom, M.; Ribacka, C.; Molin, M.; Laakkonen, L.; Verkhovsky, M.; Puustinen, A. Gating of Proton and Water Transfer in the Respiratory Enzyme Cytochrome C Oxidase. *Proc. Natl. Acad. Sci. U. S. A* **2005**, *102*, 10478−10481.
(24) Lanyi, J. K.; Schobert, B. Crystallographic Structure of the Retinal and the Protein after Deprotonation of the Schiff Base: The Switch in the Bacteriorhodopsin Photocycle *J. Mol. Biol.* **2002**, *321*, 727−737.
(25) Leiderman, P.; Huppert, D.; Agmon, N. Transition in the Temperature-Dependence of GFP Fluorescence: From Proton Wires to Proton Exit. *Biophys. J.* **2006**, *90*, 1009−1018.
(26) Belleau, B.; Conway, T.; Ahmed, F. R.; Hardy, A. D. Importance of the Nitrogen Lone Electron Pair Orientation in Stereospecific Opiates. *J. Med. Chem.* **1974**, *17*, 907−908.
(27) Kolb, V. M.; Scheiner, S. New Insights in the Clastic Binding Hypothesis for Opiate Receptor Interactions. 2. Proton-Transfer Mechanism. *J. Pharm. Sci.* **1984**, *73*, 719−723.
(28) Schobert, B.; Brown, L. S.; Lany, J. K. Crystallographic Structures of the M and N Intermediates of Bacteriorhodopsin: Assembly of a Hydrogen-Bonded Chain of Water Molecules between Asp-96 and the Retinal Schiff Base. *J. Molec. Biol.* **2003**, *330*, 553−570.
(29) Arseniev, A. S.; Barsukov, I. L.; Bystrov, V. F.; Lomize, A. L.; Ovchinnikov Yu, A. 1H-NMR Study of Gramicidin A Transmembrane Ion Channel. Head-to-Head Right-Handed, Single-Stranded Helices. *FEBS Lett.* **1985**, *186*, 168−174.
(30) Lee, Y. S.; Krauss, M. Dynamics of Proton Transfer in Bacteriorhodopsin. *J. Am. Chem. Soc.* **2004**, *126*, 2225−2230.
(31) Berezhkovskii, A.; Hummer, G. Single-File Transport of Water Molecules through a Carbon Nanotube. *Phys. Rev. Lett.* **2002**, *89*, 064503.
(32) Hassan, S. A.; Hummer, G.; Lee, Y.-S. Effects of Electric Fields on Proton Transport through Water Chains. *J. Chem. Phys.* **2006**, *124*, 204510−204518.
(33) Frisch, M. J.; Trucks, G. W.; Schlegel, H. B.; Scuseria, G. E.; Robb, M. A.; Cheeseman, J. R.; Montgomery, J. A., Jr.; Vreven, T.; Kudin, K. N.; Burant, J. C.; Millam, J. M.; Iyengar, S. S.; Tomasi, J.; Barone, V.; Mennucci, B.; Cossi, M.; Scalmani, G.; Rega, N.; Petersson, G. A.; Nakatsuji, H.; Hada, M.; Ehara, M.; Toyota, K.; Fukuda, R.; Hasegawa, J.; Ishida, M.; Nakajima, T.; Honda, Y.; Kitao, O.; Nakai, H.; Klene, M.; Li, X.; Knox, J. E.; Hratchian, H. P.; Cross, J. B.; Bakken, V.; Adamo, C.; Jaramillo, J.; Gomperts, R.; Stratmann, R. E.; Yazyev, O.; Austin, A. J.; Cammi, R.; Pomelli, C.; Ochterski, J. W.; Ayala, P. Y.; Morokuma, K.; Voth, G. A.; Salvador, P.; Dannenberg, J. J.; Zakrzewski, V. G.; Dapprich, S.; Daniels, A. D.; Strain, M. C.; Farkas, O.; Malick, D. K.; Rabuck, A. D.; Raghavachari, K.; Foresman, J. B.; Ortiz, J. V.; Cui, Q.; Baboul, A. G.; Clifford, S.; Cioslowski, J.; Stefanov, B. B.; Liu, G.; Liashenko, A.; Piskorz, P.; Komaromi, I.; Martin, R. L.; Fox, D. J.; Keith, T.; Al-Laham, M. A.; Peng, C. Y.; Nanayakkara, A.; Challacombe, M.; Gill, P. M. W.; Johnson, B.; Chen, W.; Wong, M. W.; Gonzalez, C.; Pople, J. A. *Gaussian 03*, revision B.04; Gaussian, Inc.: Pittsburgh, PA, 2003.
(34) Aceto, M. D.; Bowman, E. R.; Harris, L. S.; Hughes, L. D.; Kipps, B. R.; Lobe, S. L.; May, E. L. Dependence Studies of New Compounds in the Rhesus Monkey, Rat and Mouse. In *Problems of Drug Dependence 2005*, Proceedings of the 67th Annual Scientific Meeting, The College on Problems of Drug Dependence, Inc.; Dewey, W. L., Ed.; U.S. Department of Health and Human Services, National Institutes of Health, National Institute on Drug Abuse: Washington, D.C., 2006; NIDA Research Monograph 186, pp 188−228.
(35) Xu, H.; Hashimoto, A.; Rice, K. C.; Jacobson, A. E.; Thomas, J. B.; Carroll, F. I.; Lai, J.; Rothman, R. B. Opioid Peptide Receptor Studies. 14. Stereochemistry Determines Agonist Efficacy and Intrinsic Efficacy in the [^{35}S]GTP-γ-S Functional Binding Assay. *Synapse* **2001**, *39*, 64−69.
(36) Xu, H.; Wang, X.; Wang, J.; Rothman, R. B. Opioid Peptide Receptor Studies. 17. Attenuation of Chronic Morphine Effects after Antisense Oligodeoxynucleotide Knock-Down of RGS9 Protein in Cells Expressing the Cloned Mu Opioid Receptor. *Synapse* **2004**, *52*, 209−217.
(37) de Costa, B. R.; Iadarola, M. J.; Rothman, R. B.; Berman, K. F.; George, C.; Newman, A. H.; Mahboubi, A.; Jacobson, A. E.; Rice, K. C. Probes for Narcotic Receptor Mediated Phenomena. 18. Epimeric 6α-Iodo-3,14-dihydroxy-17-(cyclopropylmethyl)-4,5α-epoxymorphinans and 6β-Iodo-3,14-dihydroxy-17-(cyclopropylmethyl)-4,5α-epoxymorphinans as Potential Ligands for Opioid Receptor Single Photon Emission Computed Tomography−Synthesis, Evaluation, and Radiochemistry of ^{125}I-6β-Iodo-3,14-Dihydroxy-17-(cyclopropylmethyl)-4,5α-epoxymorphinan. *J. Med. Chem.* **1992**, *35*, 2826−2835.
(38) Ni, Q.; Xu, H.; Partilla, J. S.; de Costa, B. R.; Rice, K. C.; Rothman, R. B. Selective Labeling of κ_2 Opioid Receptors in Rat Brain by [^{125}I]IOXY: Interaction of Opioid Peptides and Other Drugs with Multiple κ_{2a} Binding Sites. *Peptides* **1993**, *14*, 1279−1293.
(39) *SHELXTL*, v6.10; Bruker AXS, Inc.: Madison, WI, 2000.

JM061325E